nature portfolio

Peer Review File

A concise enzyme cascade enables the manufacture of natural and halogenated protoberberine alkaloids

Corresponding Author: Professor Yijian Rao

This file contains all reviewer reports in order by version, followed by all author rebuttals in order by version.

Version 0:

Reviewer comments:

Reviewer #1

(Remarks to the Author)
An artificial enzyme cascade was developed to produce rotundine. The production of rotundine was achieved at 2.44 g L-1 through enzyme discovery and engineering, along with systematic optimization of the berberine bridge enzyme. Furthermore, this cascade facilitated the efficient biosynthesis of various unnatural halogenated protoberberine alkaloids. This work provides significant guidance for the industrial production of protoberberine alkaloid. However, additional modification may be needed to improve the manuscript as listed below before acceptance.

1. Line 53, please add the specific production titer values reported in previous studies.
2. Figure 1, the natural biosynthetic pathway of 4HPPA should be included in the Figure 2b to enable a clear comparison between natural and artificial pathway of 4HPPA and its analogues.
3. Line 268, the catalytic activity of a double mutant or triple mutant of BBE (W165G, A421F and R354W) should be evaluated.
4. Please provide the precise quantities of cofactors (ATP, Methionine and L-ascorbic acid) and substrate (1a and dopamine) supplemented throughout the entire production process of rotundine? This information should be provided in the discussion section to demonstrate the industrial production potential of rotundine. Additionally, which aspects of rotundine industrial production need further improvement in the future.

Reviewer #2

(Remarks to the Author)
The manuscript describes an enzyme cascade for production of protoberberine alkaloids, employing a modular strategy to distribute the whole pathway enzymes across four E coli strains. By combining enzyme engineering and metabolic engineering, gram-scale of Rotundine was achiveved, reaching 52.8% of the theoretical yield from substrate 2-(3-hydroxy-4-methoxyphenyl) acetic acid (1a). While many trategies utilized have been previously reported, the study presents some new insights into enzymatic catalysis through mutants of BBE and S9OMT with improved conversion efficiencies. However, several critical concerns regarding experiemntal design and data interpretation require further clarification.
Major Concerns:
1. Concerns with TfS9OMT engineering:
• Molecular docking analysis (Fig 5b):
In the docking analysis of TfS9OMT, the D-ring of substrate 7a contrasts with the crystal structures reported earlier (PDB ID: 6NEJ; ACS Catal. 2020). Given that the B and C ring of scoulerine (6a) are kinked, this orientation likely impacts the docking analysis. Could the authors elaborate on how substrate 7a interacts with the protein in this configuration?
• Impact of mutation on 9-O-methylation (Fig 5c):
The S16G/P301A mutation significantly improved conversion efficiency. Did these mutations affect the enzyme's activity for 9-O-methylation? Were any intermediates or side products, i.e., the monomethylated product tetrahydropalmatrubine (2-O-methylation), detected? Is it possible that methylation first occurs at 2-hydroxyl position before the 9- position? Further explanation on how these mutations enhance conversion efficiency is needed.
• Substrate carryover:
If the broth from the previous module was used, incomplete conversion might have left reticulin (5a) as a potential substrate

for the TfS9OMT mutants (ACS Catal. 2020). Were any side products observed in this scenario?
• Mutation of L111A:
Previous studies identified M111 of TfS9OMT as a critical residue for substrate binding and positioning, leading to a 24-fold increase of dimethylated product Rotundine (ACS Catal. 2020). However, the L111A mutation in this study negatively impacted the conversion of 7a. Was the same protein being tested? Why was this particular mutation chosen?
2. Issues with BBE engineering:
• Soluble expression of BBE (Fig S15):
The evidence provided does not confirm the formation of inclusion bodies. When expressing BBE with N-terminus truncation and an MBP tag, what controls were used? Did the total expression level of BBE increase, or was it just the soluble fraction that increased after chaperone expression?
• Amino acid conservation analysis (Fig S18a and Fig 4d):
The conservation analysis metholology is unclear. How did this guide the mutagenesis design? For example, prior research reported that the E417Q mutation led to a loss of regiospecificity (Nat Chem Biol, 2008). In this study, replacing the conserved residues R354 resulted in more than 100-fold increase in activity (Fig 4d). Could the authors provide a mechanistic explaination for this result?
• Limited yield with EcBBE mutant in vivo (Fig 4e):
Despite optimization using molecular chaperone, promoter and the FAD supply, the yield of 6a from the optimized EcBBE mutant was not that significant as shown in vitro (Fig 4d), Could the authors comment on this? Was FAD added during in vitro catalytic assays? If not, why was it a limiting factor in vivo?
3. Insufficient information regarding precursor accessibility
the study used '2-(3-hydroxy-4-methoxyphenyl) acetic acid' to bypass P450 enzymes. However, the availability and economic feasibility of this compound remain unclear. Is this precursor easily accessible and sustainable (e.g., non-oil-based)? Additional details on its sourcing and economic considerations are necessary.
Other Issues:
• Fig 2a: product 3a was formed with either "1a+Dopamine+TpCAR" or "1a+Dopamine+TpCAR+TfNCS". Does it mean the conversion of 2a and dopmine spontaneously?

Reviewer #3

(Remarks to the Author)
In this manuscript, the authors established a concise enzyme cascade for the biosynthesis of Rotundine and halogenated protoberberine alkaloid derivatives from the readily available substrates. One representative substrate is 2-(3-hydroxy-4-methoxyphenyl) acetic, which has been pre-functionalized with hydroxy and methoxy groups at C3' and C4', eliminating the need for hydroxylation by P450 NMCH and methylation by 4'-OMT. Notably, the identification of highly efficient mutants of EcBBE and S9OMT significantly enhances the conversion rates of individual modules, showcasing the industrial potential of this approach. The potency of the strategy was highlighted by the production of 2.44 g/L Rotundine and 3.19 g/L coulerine. Nevertheless, the following concerns should be fully addressed before being accepted for publication on Nature Communications.

Major Points

1. While the authors show high conversion rates of individual modules (BIA, MT, BBE, and S9OMT) separately, the overall conversion rate of the entire cascade with all modules included has not been evaluated.

2. Compound 1a and dopamine are known to undergo spontaneous Pictet-Spengler condensation without NCS. In Figure 2a, Compound 3a appears to be produced in greater amounts in the absence of TfNCS than in its presence. This raises questions about the role of TfNCS in facilitating this reaction. Including quantitative abundance information in the chromatograms would improve clarity and enable a more detailed analysis of the function of NCS.

3. When investigating the reaction order of Ps6OMT and CNMT, the authors should identify the compound formed by the CNMT reaction with substrate 3a and provide the corresponding reference standards. These details should be incorporated into Figure 2a and Supplementary Fig. 3 to make the data more solid.

4. A prior study (DOI: 10.1021/acssuschemeng.3c08493) reported that F398W-I431F mutations in AmBBE1 significantly improved catalytic activity, achieving nearly 100% conversion rates. The authors are suggested to introduce these mutations into EcBBE and compare the results with the R354W mutant. Will there be synergistic or additive effect among these mutations? Additionally, the method used to identify conserved amino acids (Line 264) should be explicitly detailed.

Minor Points

5. Line 102: "C3 and C4" should be "C3' and C4' ".

6. Line 228: "E. coli" should be italicized.

Version 1:

Reviewer comments:

Reviewer #1

(Remarks to the Author)
This revision and additional information provided have addressed my concerns. I believe this work will contribute significantly to the industrial production of protoberberine alkaloid.

Minor comment
Line 109, C3’ and C4’ should be C3′ and C4′.

Reviewer #2

(Remarks to the Author)
The authors have added more data and addresses most of my comments. However, there are still some questions remain unsloved.
As the authors mentioned, previous study (ACS Catal. 10, 4497-4509 (2020)) clearly demonstrated that leucine at position 111 was more effective than alanine for conversion of (S)-7a. What was the rational for performing the L111A mutation? Moreover, in Fig 5c, most residues were mutated to either A or G, yet some were only mutated to A. What was the reason for this selective mutation approach? A more detailed explanation of the methodology or rationale behind these choices would be valuable for protein enginering efforts.
The molecular mechanism of the R354W mutation’s effect on EcBBE activity was not entirely convincing. The authors mentioned that the distance between the C2’ carbon and the carbon atom on the N-methyl group of (S)-5a decreased. Could you provide further clarification, such as showing how this residue interact with these atoms (the C2’ carbon and the carbon atom on the N-methyl group of (S)-5a)? Additionaly, it was shown that the reaction initated by deprotonation of the C3’ OH by E417 (Nat Chem Biol, 2008). How does the R354W mutation influence this deprotonation process?

Reviewer #3

(Remarks to the Author)
The authors have done a nice job in addressing all the reviewers' concerns.

Version 2:

Reviewer comments:

Reviewer #2

(Remarks to the Author)
The authors have addressed my comments.

Response to reviewers:

Reviewer #1 (Remarks to the Author):

An artificial enzyme cascade was developed to produce rotundine. The production of rotundine was achieved at 2.44 g L^{-1} through enzyme discovery and engineering, along with systematic optimization of the berberine bridge enzyme. Furthermore, this cascade facilitated the efficient biosynthesis of various unnatural halogenated protoberberine alkaloids. This work provides significant guidance for the industrial production of protoberberine alkaloid. However, additional modification may be needed to improve the manuscript as listed below before acceptance.

A: We greatly appreciate your positive evaluations and valuable suggestions, which help us improve the quality of this manuscript. Here we prepared this point-to-point response to your concerns, which have been completely addressed, and highlighted the changes in red in the revised manuscript.

Q1: Line 53, please add the specific production titer values reported in previous studies.

A1: Thanks for your constructive advice. According to your suggestion, we have added the specific production titer values reported in previous studies in the manuscript as follows:

"However, challenges such as the complexity of their biosynthetic pathways, the difficulties in expressing plant-derived P450 enzyme and berberine bridge enzyme (BBE), and the cytotoxicity from the accumulation of alkaloids or its intermediates always results in low production titers, such as 16.9 mg L^{-1} production in berberine and 68.6 mg L^{-1} production in Rotundine in engineered yeasts, which still lack commercial viability."

Q2: Figure 1, the natural biosynthetic pathway of 4HPPA should be included in the Figure 1b to enable a clear comparison between natural and artificial pathway of 4HPPA and its analogues.

A2: Thanks for your valuable suggestion to improve the quality of this manuscript. According to your suggestion on further illustrating the comparison between natural and

artificial pathway, we have added the natural biosynthetic pathway of 4HPPA in new Figure 1b as follows:

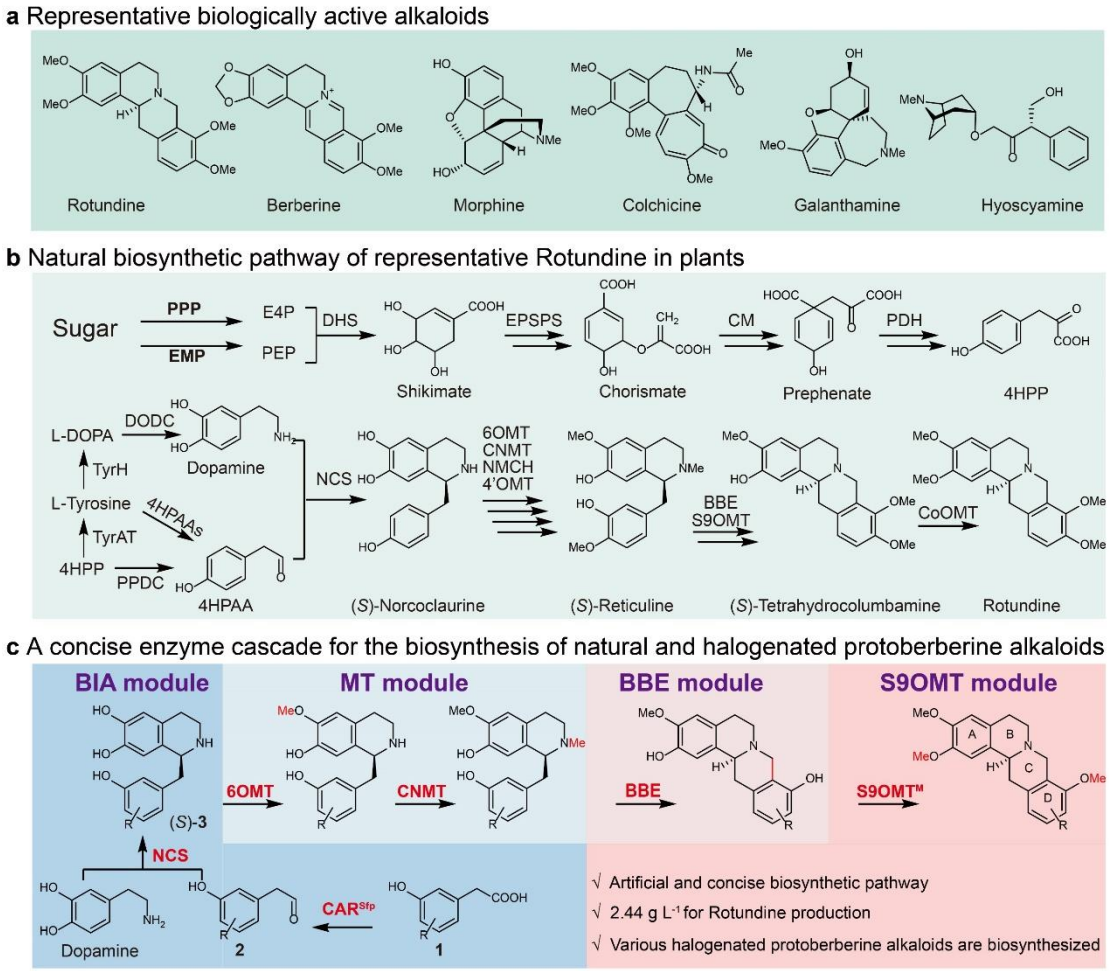

Fig. 1. Design of an artificially concise multi-enzyme cascade for the biosynthesis of natural and halogenated protoberberine alkaloids.

Q3: Line 268, the catalytic activity of a double mutant or triple mutant of BBE (W165G, A421F and R354W) should be evaluated.

A3: Thanks for your constructive suggestion on combinational mutations. According to your advice, we have evaluated the double mutants and triple mutant of BBE (*Ec*BBE-W165G/R354W, *Ec*BBE-W165G/A421F, *Ec*BBE-R354W/A421F, *Ec*BBE-W154G/R354W/A421F). Based on the *in vitro* assays, the tested combinational mutations exhibited worse performance than *Ec*BBE-R354W, thus we still chose *Ec*BBE-R354W mutant (*Ec*BBE#) for subsequent tests.

These results have been added in Supplementary Fig. 20 as follows:

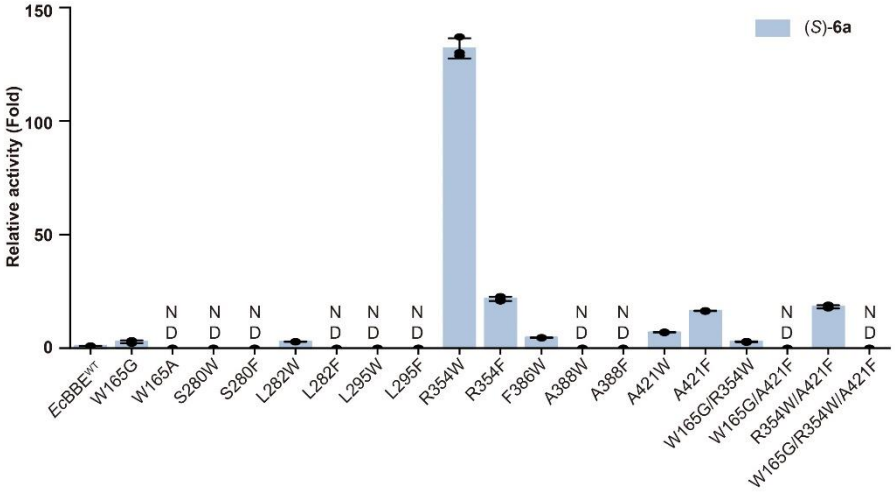

Supplementary Figure 20. Relative activity of all mutants of *Ec*BBE^{WT} toward (*S*)-5a *in vitro*. The relative activity is defined as the ratio of the (*S*)-**6a** titer of *Ec*BBE^{WT} mutants to that of *Ec*BBE^{WT}. ND: not detected.

Q4-1: Please provide the precise quantities of cofactors (ATP, Methionine and L-ascorbic acid) and substrate (**1a** and dopamine) supplemented throughout the entire production process of rotundine? This information should be provided in the discussion section to demonstrate the industrial production potential of rotundine.

Q4-2: Additionally, which aspects of rotundine industrial production need further improvement in the future.

A4: Thanks for your valuable suggestion on the industrial production potential of rotundine. As you suggest, we have added the sentences in the revised manuscript of the **discussion** section as follows:

"In this concise enzyme cascade, 13 mM **1a**, 18.2 mM dopamine, 60 mM ATP, 60 mM L-Methionine and 40 mM L-ascorbic acid sodium salt were used to prepare Rotundine, achieving 52.8 % of the theoretical yield of **1a**. For the industrial biosynthesis of natural and halogenated protoberberine alkaloids, further engineering of BBE and *Tf*S9OMT# is required. Additionally, the stability of all enzymes should be considered to enable their recycling and reduce costs."

Reviewer #2 (Remarks to the Author):

The manuscript describes an enzyme cascade for production of protoberberine alkaloids, employing a modular strategy to distribute the whole pathway enzymes across four E coli strains. By combining enzyme engineering and metabolic engineering, gram-scale of Rotundine was achiveved, reaching 52.8% of the theoretical yield from substrate 2-(3-hydroxy-4-methoxyphenyl) acetic acid (**1a**). While many strategies utilized have been previously reported, the study presents some new insights into enzymatic catalysis through mutants of BBE and S9OMT with improved conversion efficiencies. However, several critical concerns regarding experiemntal design and data interpretation require further clarification.

A: We would like to thank your professional feedbacks and constructive suggestions, which effectively help us improve the quality of this manuscript. Here we prepared this point-to-point response to your concerns, which have been completely addressed, and highlighted the changes in red in the revised manuscript.

Major Concerns:

Q1: Concerns with *Tf*S9OMT engineering:

• Molecular docking analysis (Fig 5b):

In the docking analysis of TfS9OMT, the D-ring of substrate **7a** contrasts with the crystal structures reported earlier (PDB ID: 6NEJ; ACS Catal. 2020). Given that the B and C ring of scoulerine (**6a**) are kinked, this orientation likely impacts the docking analysis. Could the authors elaborate on how substrate **7a** interacts with the protein in this configuration?

A1: We apologize for the unclear presentation of Fig. 5b. According to your constructive suggestion to avoid the indiscernible and kinked structure of substrate in three-dimensional schemes, we have elaborated the molecular interactions of (*S*)-**6a** with *Tf*S9OMT and (*S*)-**7a** with *Tf*S9OMT^{M} (*Tf*S9OMT-M111L/N191D/F205S) through the two-dimensional docking diagrams for clear presentation, which have also been added in Supplementary Fig. 25 as follows:

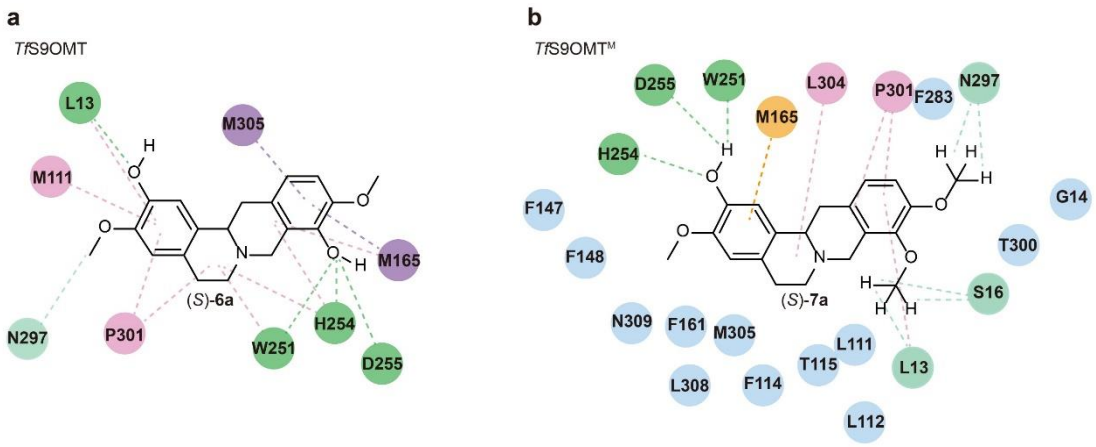

Supplementary Figure 25. Two-dimensional docking diagram and molecular interactions of (*S*)-6a with *Tf*S9OMT and (*S*)-7a with *Tf*S9OMT^{M}. a Two-dimensional docking diagram and molecular interactions of (*S*)-**6a** with *Tf*S9OMT. **b** Two-dimensional docking diagram and molecular interactions of (*S*)-**7a** with *Tf*S9OMT^{M}. Van der Waals: light blue, conventional hydrogen bond: green, carbon hydrogen bond: cyan, π-sulfur: orange, π-alkyl: pink, π-sigma: purple.

Q2: • Impact of mutation on 9-*O*-methylation (Fig 5c):

1: The S16G/P301A mutation significantly improved conversion efficiency. Did these mutations affect the enzyme's activity for 9-*O*-methylation?

2: Were any intermediates or side products, i.e., the monomethylated product tetrahydropalmatrubine (2-*O*-methylation), detected? Is it possible that methylation first occurs at 2-hydroxyl position before the 9- position?

3: Further explanation on how these mutations enhance conversion efficiency is needed.

A2-1: Thanks for your constructive comment. To further explain the process of the reaction catalyzed by *Tf*S9OMT^{M}-S16G/P301A (*Tf*S9OMT#), we have analyzed the reaction *in vitro* in detail (Supplementary Fig. 27). In the successive two-staged methylation, unreacted substrate (*S*)-**6a** was found in the *in vitro* assay of *Tf*S9OMT^{M}, while no obvious accumulation of (*S*)-**6a** was found in the reaction of *Tf*S9OMT#, indicating the mutant *Tf*S9OMT# not only improved the total conversion efficiency of the two-staged methylation, but also improved the enzyme's activity for 9-*O*-methylation for the undetected (*S*)-**6a** in the reaction mixture of *Tf*S9OMT#.

The description has also been added in the revised manuscript as follows.

"After combinational mutagenesis, a double mutant *Tf*S9OMT^{M}-S16G/P301A

(*Tf*S9OMT#) showed a 19-fold increase in catalytic activity compared to *Tf*S9OMT^{M} (Fig. 5c, Supplementary Fig. 27), without the decrease of catalytic activity for the first 9-*O*-methylation process."

A2-2: Thanks for your professional comment. We have further carefully analyzed HPLC profile during the process of (*S*)-**6a** catalyzed by *Tf*S9OMT# (Supplementary Fig. 28). Except for the major intermediate (*S*)-**7a**, another new product with trace amount was discovered, which could subsequently be transformed to Rotundine ((*S*)-**8a**). Thus, the new product was postulated as the monomethylated product (*S*)-tetrahydropalmatrubine ((*S*)-**7a'**), also according to the previous study (Valentic, T. R. et al. *ACS Catal.* **10**, 4497-4509 (2020)).

Therefore, Rotundine could be generated by *Tf*S9OMT# through two paths: 1) the methylation occurs firstly at 9-hydroxyl position and then at 2-position; 2) the methylation firstly occurs at 2-hydroxyl position, and subsequently at the 9-position, and path 1 was dominant due to the larger amount of (*S*)-**7a** than (*S*)-**7a'** observed in HPLC assays. These results have also been added in the revised manuscript and Supplementary Information as follow.

"without the decrease of catalytic activity for the first 9-*O*-methylation process. During the two-staged methylation process, another intermediate postulated as (*S*)-tetrahydropalmatrubine ((*S*)-7a') might be formed through initial methylation at 2-hydroxyl position, indicating that both pathways with different methylation sequences are possible (Supplementary Fig. 28), but without affecting the production of Rotundine."

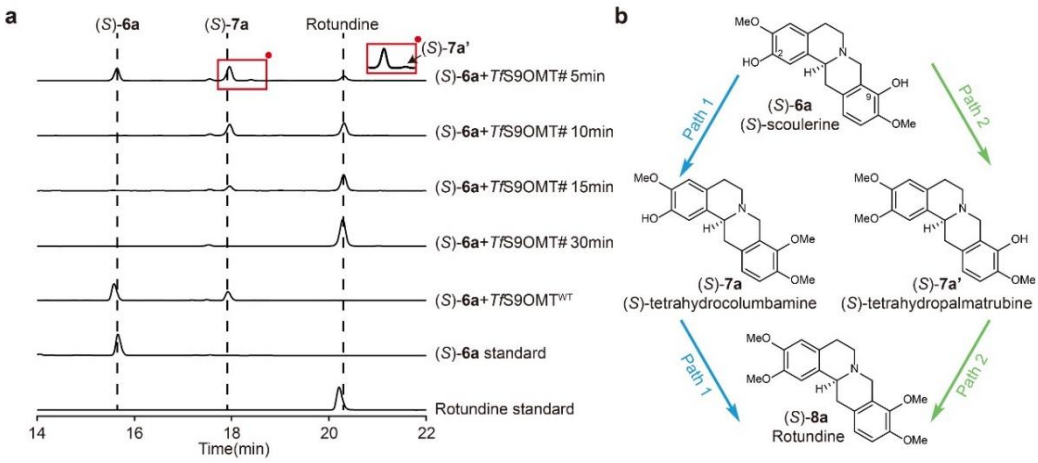

Supplementary Figure 28. Potential catalytic pathways study of *Tf*S9OMT#. a HPLC analysis *in vitro* assays of *Tf*S9OMT#. The new product (postulated as (*S*)-**7a'**) was observed when enlarging the spectrum highlighted in red rectangle. **b** Two putative paths of Rotundine synthesis by *Tf*S9OMT#. Pathway 1 highlighted in blue involves the methylation first occurs at 9-hydroxyl position before the 2-position. Pathway 2 highlighted in green involves the methylation first occurs at 2-hydroxyl position before the 9-position.

A2-3: Thanks for your valuable question. The kinetic analysis of the mutant is most intuitive method to explain the enhanced conversion, however, it is difficult to calculate the k_{cat}/K_m considering that the reaction of *Tf*S9OMT# is a successive two-staged methylation process. Therefore, the volume of substrate-binding pocket and binding free energy, instead of kinetic parameters, were calculated to further explain the enhanced activity of *Tf*S9OMT# in Supplementary Fig. 29. These results indicate that the *Tf*S9OMT# mutant can not only create a larger substrate pocket, but also decrease the binding free energy than *Tf*S9OMT^{M}, allowing for better substrate binding.

The corresponding description has been added in the revised manuscript, and the added Supplementary Fig. 29 has also been attached as follows:

"Molecular docking results suggest that the improved catalytic activity may be due to a larger substrate pocket and lower binding free energy of TfS9OMT# compared to TfS9OMT^{M}, allowing for better substrate binding (Supplementary Fig. 29)."

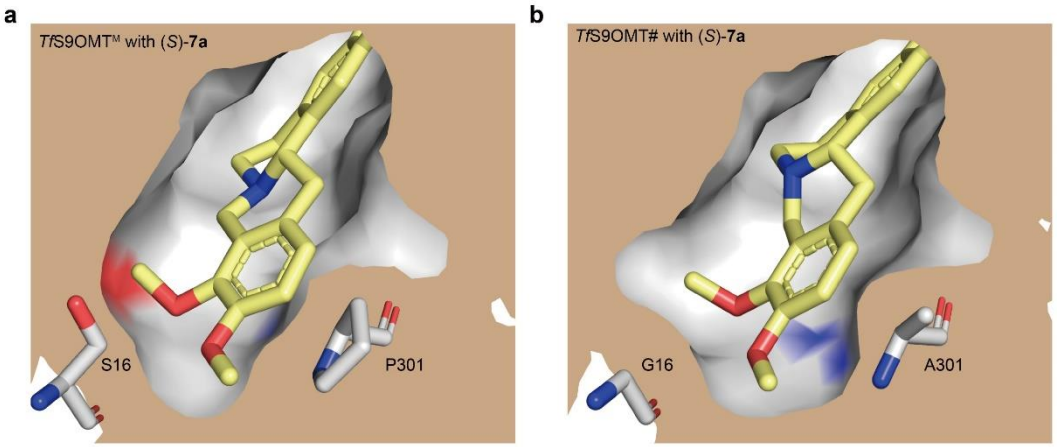

c

	Interaction energy between substrate and 4 Å protein residues (including SAM)	The volume of substrate-binding pocket
*Tf*S9OMT^{M} with (*S*)-**7a**	-50.62176 kcal/mol	647 Å^3
*Tf*S9OMT# with (*S*)-**7a**	-52.71836 kcal/mol	668 Å^3

Supplementary Figure 29. Cross-section of the substrate binding pocket of *Tf*S9OMT. a Substrate binding site highlighted in cross-section of *Tf*S9OMT^{M}. **b** Substrate binding site

highlighted in cross-section of *Tf*S9OMT#. **c** The calculation of the interaction energy between (*S*)-**7a** and 4 Å protein residues of *Tf*S9OMT (including SAM) and the volume of substrate-binding pocket.

Q3: • Substrate carryover:

If the broth from the previous module was used, incomplete conversion might have left reticuline (**5a**) as a potential substrate for the *Tf*S9OMT mutants (ACS Catal. 2020). Were any side products observed in this scenario?

A3: Thanks for your professional question. As the previous study (Valentic, T. R. et al. *ACS Catal.* **10**, 4497-4509 (2020)) reported that *Tf*S9OMT mutants could catalyze (*S*)-reticuline ((*S*)-**5a**) to two products ((*S*)-codamine and (*S*)-laudanine), we tested our optimal mutant *Tf*S9OMT#, and found it could also transform (*S*)-**5a** to two new products (postulated as (*S*)-codamine and (*S*)-laudanine) *in vitro*, which is consistent with the previous study.

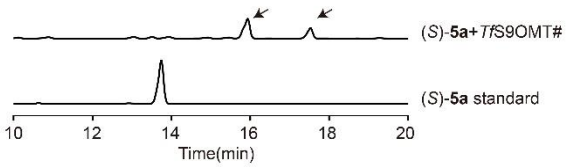

However, the production of by-products could hardly be observed during the multi-enzyme cascade, because the temporal separation strategy between different modules was employed in the whole-cell system. Additionally, (*S*)-**5a** was almost completely transformed to (*S*)-**6a** in BBE module (Fig. 4f, Supplementary Fig. 32), which could not be catalyzed by *Tf*S9OMT# in the next module to produce side-products. All these reasons lead to the difficult observation of side-products in this scenario.

The results have also been added as Supplementary Fig. 32 in the revised Supplementary Information.

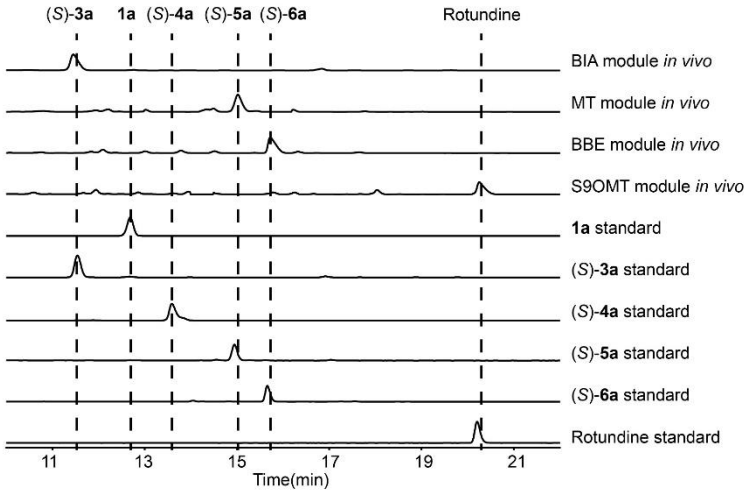

Supplementary Figure 32. Establishment of a multi-enzyme cascade reaction to efficiently synthesize Rotundine in whole-cell reaction system.

Q4: • Mutation of L111A:

Previous studies identified M111 of *Tf*S9OMT as a critical residue for substrate binding and positioning, leading to a 24-fold increase of dimethylated product Rotundine (ACS Catal. 2020). However, the L111A mutation in this study negatively impacted the conversion of **7a**. Was the same protein being tested? Why was this particular mutation chosen?

A4: We apologize for the unclear description. At first, the same protein was used in this study. The mutant we tested was *Tf*S9OMT-M111L/N191D/F205S (*Tf*S9OMT^{M}), and the L111A mutation negatively impacted the conversion of (*S*)-**7a**, indicating leucine was better than alanine at 111 position in our study (Fig. 5c). In fact, in the previous study (Figure 6B in *ACS Catal.* **10**, 4497-4509 (2020)), *Tf*S9OMT-M111L/N191D/F205S (*Tf*S9OMT^{M}) also showed higher activity than *Tf*S9OMT-M111A/N191D/F205S to produce Rotundine *in vivo*, indicating that leucine is better than alanine at 111 position. Thus, our result is similar to the previous study.

In order to avoid the misunderstanding by other readers, we changed the description in the revised manuscript as follows:

"As a result, the mutants *Tf*S9OMT^{M}-S16G, *Tf*S9OMT^{M}-T115A, *Tf*S9OMT^{M}-P301G and *Tf*S9OMT^{M}-P301A showed 11-fold, 5-fold, 12-fold and 13-fold increases in the transformation of (*S*)-**6a** to (*S*)-**8a** compared with *Tf*S9OMT^{M}, respectively[28].**"**

Q5: Issues with BBE engineering:

• Soluble expression of BBE (Fig S15):

The evidence provided does not confirm the formation of inclusion bodies. When expressing BBE with *N*-terminus truncation and an MBP tag, what controls were used? Did the total expression level of BBE increase, or was it just the soluble fraction that increased after chaperone expression?

A5: Thanks for your very professional advice. According to your suggestions, we have used the cell lysates/ supernatant/ pellet of expressed *Ec*BBE without *N*-terminal signal peptide truncation or a solubilizing tag (MBP) as the control, to retest the expression of *Ec*BBE. The results (updated Supplementary Fig. 16a) showed that the *N*-terminal signal peptide truncation and solubilizing tag (MBP) on *Ec*BBE could increase both of the total and the soluble expression level of *Ec*BBE. However, we all know that increased soluble expression of proteins does not mean that they are all correctly folded with increased activities, so we tried to co-express molecular chaperones with *Ec*BBE to further improve the titer of (*S*)-**6a**. Considering the increased production of (*S*)-**6a** through co-expressing the chaperone Gro7 with *Ec*BBE in M3g (Supplementary Fig. 17), we compared the protein expression of strains with/without molecular chaperones to further elucidate the role of molecular chaperones in BBE expression (Supplementary Fig. 16b). It showed that the molecular chaperon increased not only the activity but also solubility of *Ec*BBE.

Therefore, we updated Supplementary Fig. 16, and corrected the misleading description of BBE expression in the revised manuscript as follows:

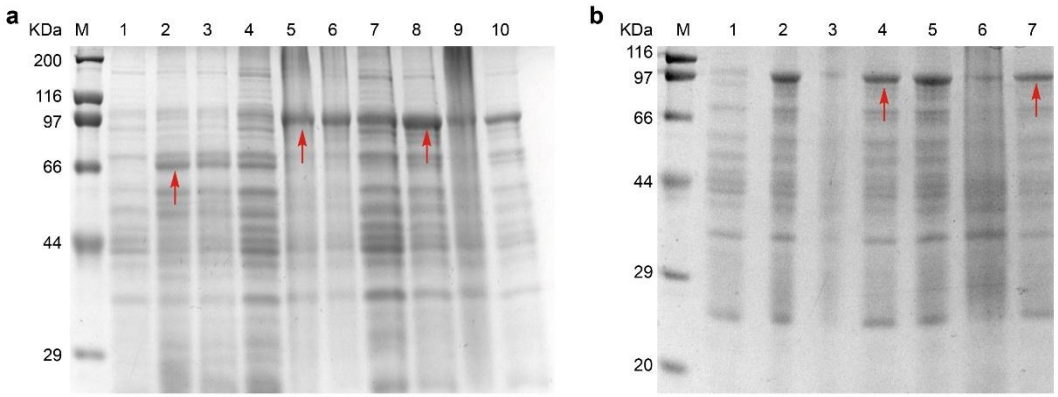

Supplementary Figure 16. SDS-PAGE analysis of *Ec*BBE with *N*-terminal signal peptide truncation and a solubilizing tag (MBP) expressed in *E. coli* BL21 (DE3). a M:

marker; lane 1: no IPTG induction; lane 2: cell lysates expressing *Ec*BBE using vector pet21b; lane 3: the pellet of cell lysates expressing *Ec*BBE using vector pet21b; lane 4: the supernatant of cell lysates expressing *Ec*BBE using vector pet21b; lane 5: cell lysates expressing *Ec*BBE with *N*-terminal signal peptide truncation and a solubilizing tag (MBP) using vector pet21b; lane 6: the pellet of cell lysates expressing *Ec*BBE with *N*-terminal signal peptide truncation and a solubilizing tag (MBP) using vector pet21b; lane 7: the supernatant of cell lysates expressing *Ec*BBE with *N*-terminal signal peptide truncation and a solubilizing tag (MBP) using vector pet21b; lane 8: cell lysates expressing *Ec*BBE with *N*-terminal signal peptide truncation and a solubilizing tag (MBP) using vector pCDFDuet in M3d; lane 9: the pellet of cell lysates expressing *Ec*BBE with *N*-terminal signal peptide truncation and a solubilizing tag (MBP) using vector pCDFDuet in M3d; lane 10: the supernatant of cell lysates expressing *Ec*BBE with *N*-terminal signal peptide truncation and a solubilizing tag (MBP) using vector pCDFDuet in M3d. Target proteins in the cell lysates are indicated by red arrows. **b** M: marker; lane 1: no IPTG induction; lane 2: cell lysates of M3g; lane 3: the pellet of cell lysates of M3g; lane 4: the supernatant of cell lysates of M3g; lane 5: cell lysates of M3d; lane 6: the pellet of cell lysates of M3d; lane 7: the supernatant of cell lysates of M3d. Target proteins in the supernatant are indicated by red arrows.

"To improve the titer of (*S*)-**6a** by increasing the soluble and functional expression levels of *Ec*BBE, we first carried out *N*-terminal signal peptide truncation, a solubilizing tag (MBP) fused with *Ec*BBE, and the strains optimization with different plasmids (M3b- M3e). It showed that the yield of (*S*)-**6a** was improved to 5.3% using strain M3d (Fig. 4b) with increased total and soluble expression level of *Ec*BBE (Supplementary Fig. 16a), but still remained very low. This could be attributed to the lack of an auxiliary protein folding mechanism in *E. coli* for plant-derived enzymes, as part of MBP-*Ec*BBE still existed in the form of inclusion bodies (Supplementary Fig. 16a)."

Q6: • Amino acid conservation analysis (Fig S18a and Fig 4d):

1: The conservation analysis methodology is unclear. How did this guide the mutagenesis design? For example, prior research reported that the E417Q mutation led to a loss of regiospecificity (Nat Chem Biol, 2008).

2: In this study, replacing the conserved residues R354 resulted in more than 100-fold increase in activity (Fig 4d). Could the authors provide a mechanistic explanation for this result?

A6-1: We feel very sorry for the misleading description. Detailed information was firstly

added in figure legend of Supplementary Fig. 19, which has been listed as follows.

"A total of 100 sequences exhibiting at least 50% identity with *Ec*BBE were generated using BLAST tools available through NCBI. Sequence alignment was conducted using BioEdit, and the regions of interest were visualized using WebLogo."

According to the previous literature (Capra, J. A., & Singh, M. *Bioinformatics*. **23**, 1875-1882 (2007)), conserved amino acids often affect ligand binding, protein-protein interaction interfaces, maintain structure, and determine protein functional specificity seriously, which could provide evidence for mutagenesis design. Therefore, Y106 and F356 as the most conserved amino acids were maintained in the work. Meanwhile, although D352, N390, and E417 are not strictly conserved, they were also maintained because of the formation of hydrogen bonds with the hydroxyl or methoxy groups of (*S*)-**5a**, which might be crucial for the substrate binding. Thus, this strategy could assist the mutant design, which was corrected from the misleading description on "conservation analysis guide the mutagenesis design". The revised description in manuscript was listed as follows.

"Thus, residues within 4.0 Å of (*S*)-**5a** were mutated with the exception of Y106 and F356 identified as conserved amino acids crucial for maintaining structural stability (Supplementary Fig. 19a), as well as D352, N390, and E417 forming hydrogen bonds with the hydroxyl or methoxy groups of (*S*)-**5a** for substrate binding (Supplementary Fig. 19b). Then, S280, L282, L295, R354, F386, A388, and A421 were mutated to tryptophan or phenylalanine to introduce steric hindrance, while W165 was mutated to alanine or glycine to reduce steric hindrance (Fig. 4c)."

A6-2: Thanks for your valuable suggestion. Molecular dynamics studies were performed to further explain the increased catalytic activity of *Ec*BBE#. It was observed that the mean RMSD values (1.62 Å) and the mean RMSF values (0.63 Å) for 100 ns of *Ec*BBE# were lower than those of *Ec*BBE^{WT} (1.97 Å and 0.81 Å), respectively, indicating the increased protein stability of *Ec*BBE# (Supplementary Fig. 22a, 22b). Meanwhile, the distance between the C2' carbon and the carbon atom on the *N*-methyl group of (*S*)-**5a** decreased

from 4.19 Å to 3.64 Å, which favored the formation of the C-C bond of (*S*)-**6a**, while the distance between substrate and FAD was essentially unchanged (Supplementary Fig. 22c, 22d). These results well explained the increased catalytic activity of *Ec*BBE# for improved protein stability and shorter distance between reaction sites, which has been added in the revised manuscript as follows. In addition, new Supplementary Fig. 22 was provided.

"which improved the protein stability and shortened the distance between the C2' carbon and the carbon atom on the *N*-methyl group of (*S*)-**5a** (from 4.19 Å to 3.64 Å) rather than the distance between the carbon atom on the *N*-methyl group of (*S*)-**5a** and N5 atom of FAD (Supplementary Fig. 22)."

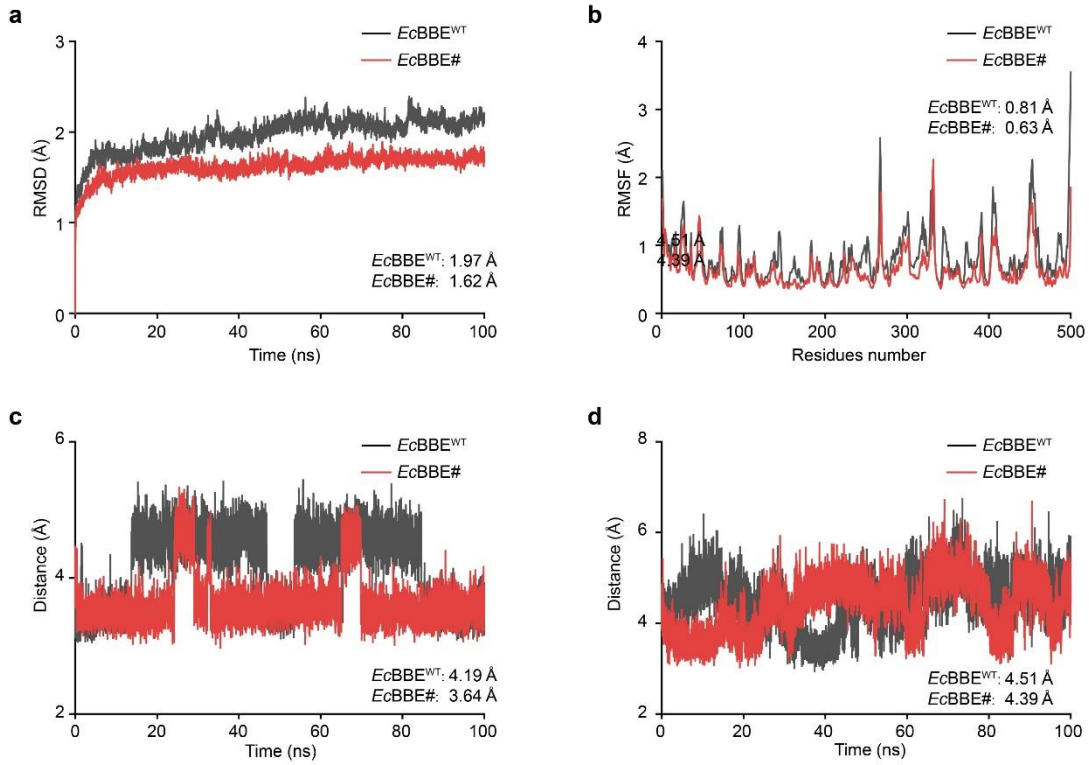

Supplementary Figure 22. Molecular dynamics simulation analysis for wild type *Ec*BBE (black) and mutant *Ec*BBE# (red). a Root mean square deviation (RMSD). **b** Root mean square fluctuation (RMSF). **c** The distance between the C2' carbon and the carbon atom on the *N*-methyl group of (*S*)-**5a**. **d** The distance between the carbon atom on the *N*-methyl group of (*S*)-**5a** and N5 atom of FAD.

Q7: • Limited yield with *Ec*BBE mutant *in vivo* (Fig 4e):

Despite optimization using molecular chaperone, promoter and the FAD supply, the yield of **6a** from the optimized *Ec*BBE mutant was not that significant as shown *in vitro* (Fig 4d),

Could the authors comment on this? Was FAD added during *in vitro* catalytic assays? If not, why was it a limiting factor *in vivo*?

A7: Thanks for your professional suggestion. You are right. This is very likely due to the differences in conditions between *in vitro* and *in vivo* assays, such as variations in protein purity and cofactor concentration. Therefore, the observed difference in the increased activity of the *Ec*BBE# mutant *in vivo* does not fully align with its *in vitro* performance, which is similar to the previous study (*ACS Catal.* **10**, 4497-4509 (2020)).

In addition, purified *Ec*BBE carries a covalently attached FAD cofactor based on previous study (Winkler, A. et. al. *J Biol Chem* **281**, 21276-21285 (2006)), indicating that the addition of FAD was not necessary for the *in vitro* assay. In fact, *in vitro* enzymatic assays, no FAD was added in our experiment. However, given that the addition of FAD during the in whole-cell reaction system improved product generation (Supplementary Fig. 23), implying an insufficient FAD supply *in vivo* due to the optimized protein expression. Thus, an FAD supply system was constructed to further improve product generation.

We have also added the corresponding description in the revised manuscript.

"By introducing the FAD supply pathway for BBE into M3y, including *RibH*, *RibF* and *RibC*, the resulting strain M3z further increased the yield of (*S*)-**6a** to 57.3% (Fig. 4e, Supplementary Fig. 23), similar to the reaction system with the extra addition of FAD."

Q8: Insufficient information regarding precursor accessibility

the study used '2-(3-hydroxy-4-methoxyphenyl) acetic acid' to bypass P450 enzymes. However, the availability and economic feasibility of this compound remain unclear. Is this precursor easily accessible and sustainable (e.g., non-oil-based)? Additional details on its sourcing and economic considerations are necessary.

A8: Thanks for your constructive advice. The substrate 2-(3-hydroxy-4-methoxyphenyl) acetic acid (**1a**) used in this work is readily purchased from Energy Chemical (Shanghai, China) at the price of 267USD/100g. The details on its sourcing have been added in the revised **Methods** section as follows.

"2-(3-hydroxy-4-methoxyphenyl) acetic acid (**1a**) was purchased from Energy Chemical (Shanghai, China). All other reagents and solvents used in this study were

purchased from China National Pharmaceutical Group Corp (Shanghai, China), Aladdin (Shanghai, China) and Macklin (Shanghai, China) (Supplementary Table 1)."

Other Issues:

Q9: Fig 2a: product **3a** was formed with either "**1a**+Dopamine+TpCAR" or "**1a**+Dopamine+*Tp*CAR+*Tf*NCS". Does it mean the conversion of **2a** and dopamine spontaneously?

A9: Thanks for your professional question. Compound **2a** catalyzed by *Tp*CAR from **1a** is known to undergo spontaneous Pictet-Spengler condensation with dopamine, as previous reported (Pesnot, T. et. al. *Chem. Commun.* **47**, 3242-3244 (2011)) to produce racemic **3a**, while the introduction of *Tf*NCS could produce (*S*)-**3a** with very high enantioselectivity (Sheng, X. et. al. *J Am Chem Soc* **141**, 11230-11238 (2019)), which was also supported by our new experimental results (Supplementary Fig. 2).

In addition, to avoid misinterpretation of the necessity of *Tf*NCS in the Pictet-Spengler reaction, we further analyzed the chirality of (*S*)-**3a** to further reflect the role of *Tf*NCS in Supplementary Fig. 2. Chiral HPLC analysis showed that (*S*)-**3a** was prepared with >99% *ee*, illustrating the high stereocontrol of *Tf*NCS. The revised and newly added results are presented in Fig. 2a and Supplementary Fig. 2, respectively, which are also listed as follows:

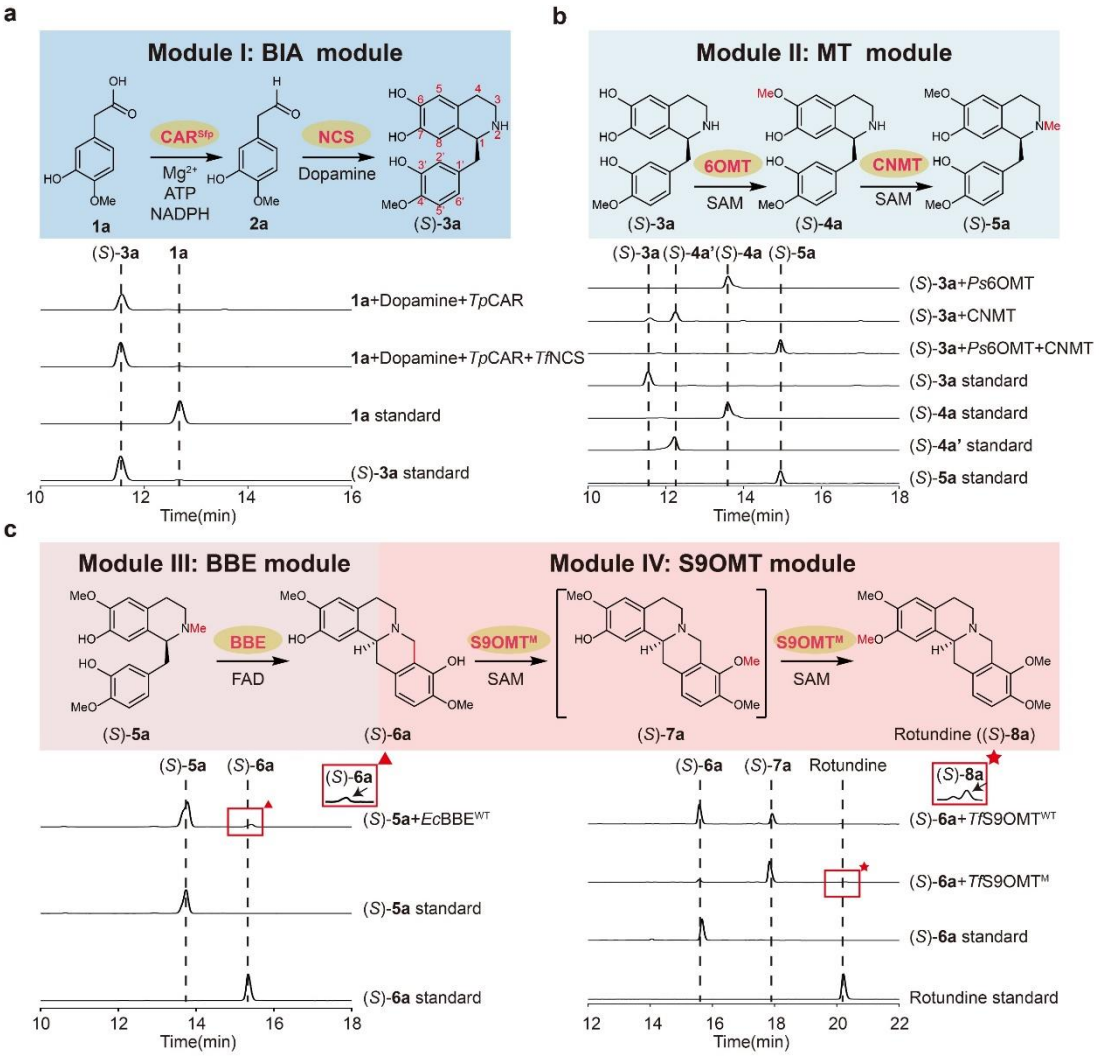

Fig. 2. Establishment of a multi-enzyme cascade reaction to efficiently synthesize Rotundine *in vitro*.

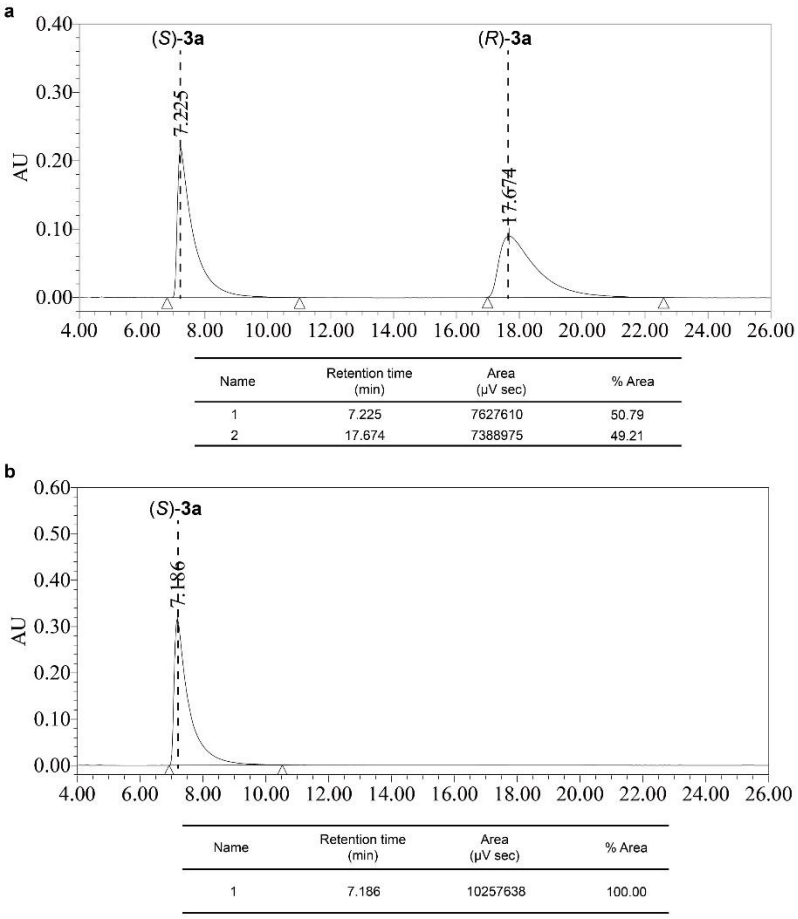

Name	Retention time (min)	Area (μV sec)	% Area
1	7.225	7627610	50.79
2	17.674	7388975	49.21

Name	Retention time (min)	Area (μV sec)	% Area
1	7.186	10257638	100.00

Supplementary Figure 2. Enantioselectivity analysis of *Tf*NCS. a Chiral HPLC analysis of (*rac*)-**3a** synthesized by *Tp*CAR. **b** Chiral HPLC analysis of (*S*)-**3a** synthesized by *Tp*CAR and *Tf*NCS. The enantioselectivities were analyzed via HPLC on a chiral stationary phase. HPLC: Chiral Pak® CHIRALCEL OD-H, n-hexane/isopropanol/diethylamine 75/25/0.1, flow rate = 1.2 mL/min, uv-vis λ =280 nm, t_{R1} = 7.2 min.

Reviewer #3 (Remarks to the Author):

In this manuscript, the authors established a concise enzyme cascade for the biosynthesis of Rotundine and halogenated protoberberine alkaloid derivatives from the readily available substrates. One representative substrate is 2-(3-hydroxy-4-methoxyphenyl) acetic, which has been pre-functionalized with hydroxy and methoxy groups at C3' and C4', eliminating the need for hydroxylation by P450 NMCH and methylation by 4'-OMT. Notably, the identification of highly efficient mutants of EcBBE and S9OMT significantly enhances the conversion rates of individual modules, showcasing the industrial potential of this

approach. The potency of the strategy was highlighted by the production of 2.44 g/L Rotundine and 3.19 g/L coulerine. Nevertheless, the following concerns should be fully addressed before being accepted for publication on Nature Communications.

A: We would like to thank the reviewer for the thoughtful comments and constructive suggestions, which help us improve the quality of this manuscript. Here we prepared this point-to-point response to your concerns, which have been completely addressed, and highlighted the changes in red in the revised manuscript.

Major Points

Q1: While the authors show high conversion rates of individual modules (BIA, MT, BBE, and S9OMT) separately, the overall conversion rate of the entire cascade with all modules included has not been evaluated.

A1: Thanks for your constructive suggestion. In this study, the conversion rates of all intermediates and final product Rotundine was calculated by using the starting substrate **1a** as the reference. So, the overall conversion rate of the entire cascade with all modules has been calculated in the manuscript as the molar concentration of intermediates or products divided by the molar concentration of substrate (**1a**), which has been shown in the revised manuscript as follows.

"Under optimal conditions of pH 8.0, 40 ^{o}C and an OD_{600} of 21 of strain concentration, strain M4b produced Rotundine at a remarkable gram-scale titer of 2.44 g L^{-1}. The overall production of Rotundine represented 52.8 % of the theoretical yield of **1a** (Fig. 5f, Supplementary Fig. 31), over 35 times higher than the previously reported yield.**"**

And also shown in the **DISCUSSION** section.

"In this concise enzyme cascade, 13 mM 1a, 18.2 mM dopamine, 60 mM ATP, 60 mM L-Methionine and 40 mM L-ascorbic acid sodium salt were used to prepare Rotundine, achieving 52.8 % of the theoretical yield of 1a."

Q2: Compound **1a** and dopamine are known to undergo spontaneous Pictet-Spengler

condensation without NCS. In Figure 2a, Compound **3a** appears to be produced in greater amounts in the absence of *Tf*NCS than in its presence. This raises questions about the role of *Tf*NCS in facilitating this reaction. Including quantitative abundance information in the chromatograms would improve clarity and enable a more detailed analysis of the function of NCS.

A2: Thanks for your significantly valuable advice. To avoid misinterpretation of the necessity of *Tf*NCS in the Pictet-Spengler reaction, we further analyzed the chirality of (*S*)-**3a** to further reflect the role of *Tf*NCS in Supplementary Fig. 2. Chiral HPLC analysis showed that (*S*)-**3a** was prepared with >99% *ee*, illustrating the high stereocontrol of *Tf*NCS. However, only racemic **3a** was produced without the addition of *Tf*NCS. The revised and newly added results are presented in Fig. 2a and Supplementary Fig. 2, respectively, which are also listed as follows:

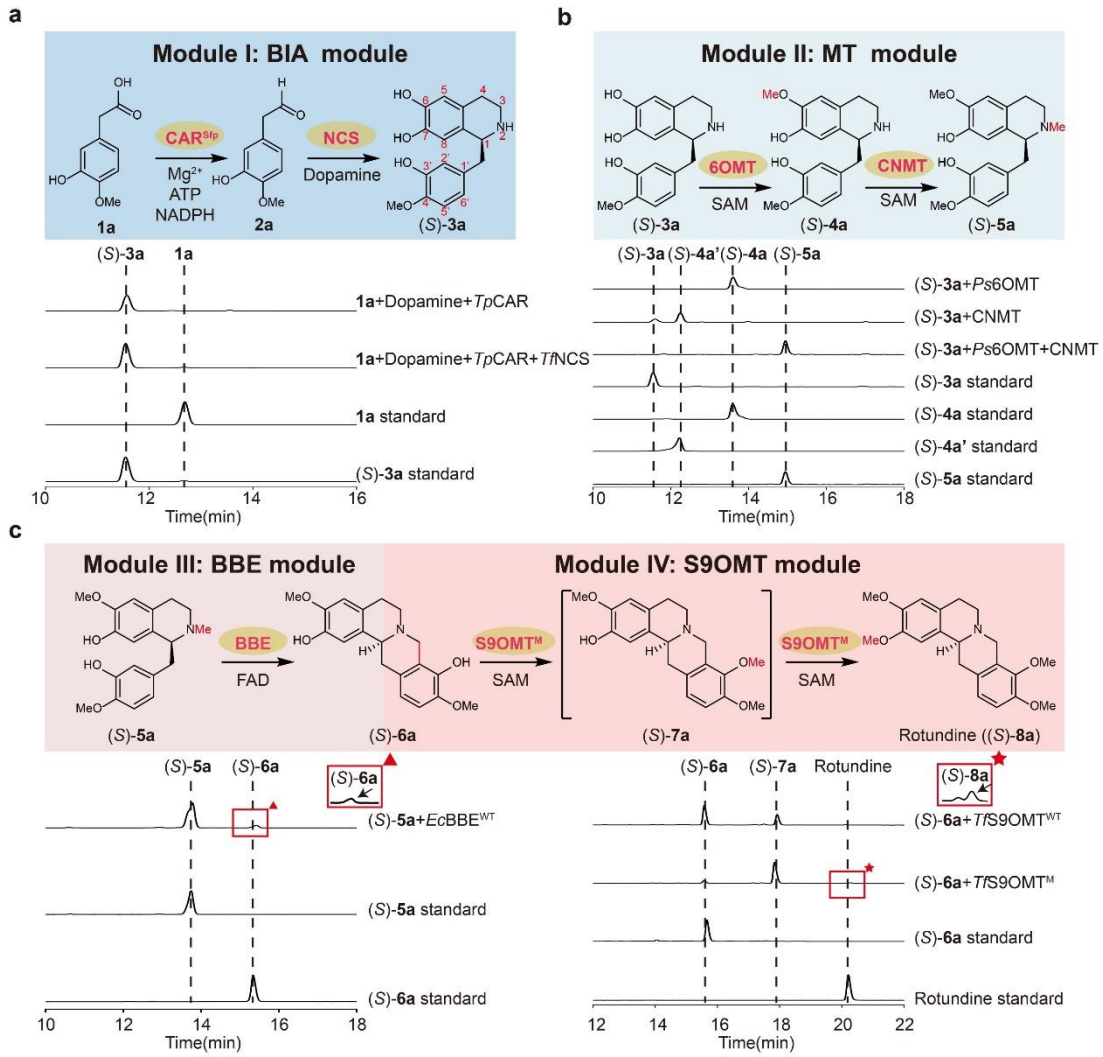

Fig. 2. Establishment of a multi-enzyme cascade reaction to efficiently synthesize Rotundine *in vitro*.

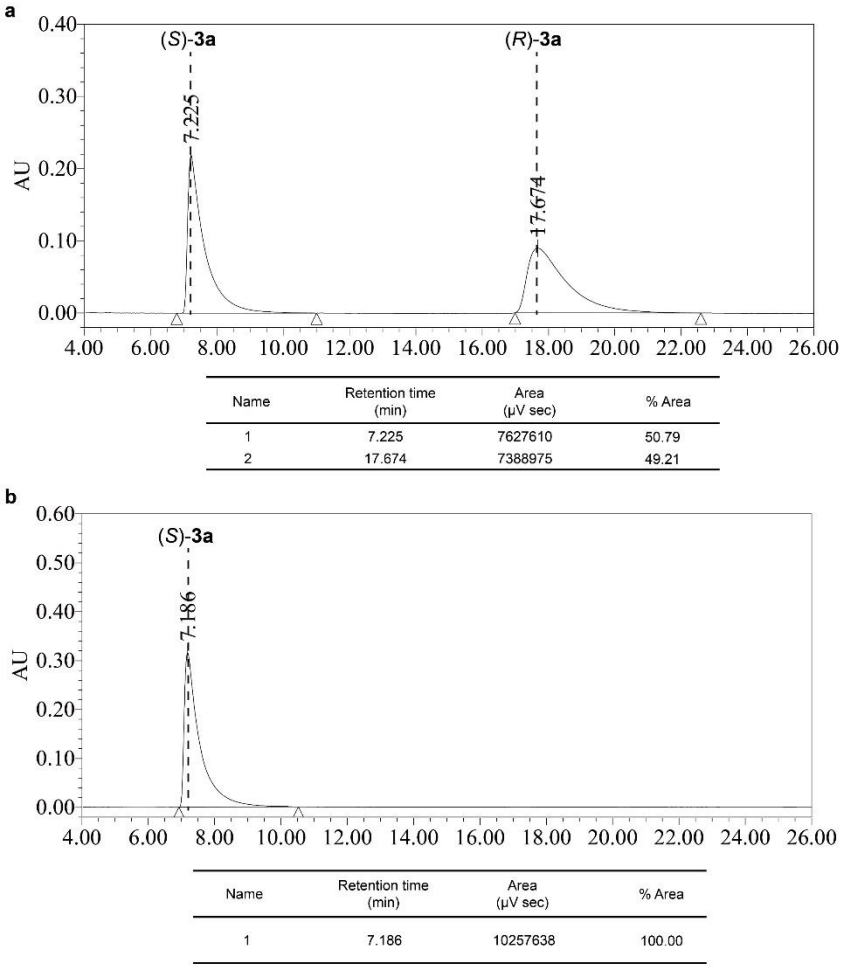

Name	Retention time (min)	Area (μV sec)	% Area
1	7.225	7627610	50.79
2	17.674	7388975	49.21

Name	Retention time (min)	Area (μV sec)	% Area
1	7.186	10257638	100.00

Supplementary Figure 2. Enantioselectivity analysis of *Tf*NCS. a Chiral HPLC analysis of (*rac*)-**3a** synthesized by *Tp*CAR. **b** Chiral HPLC analysis of (*S*)-**3a** synthesized by *Tp*CAR and *Tf*NCS. The enantioselectivities were analyzed via HPLC on a chiral stationary phase. HPLC: Chiral Pak® CHIRALCEL OD-H, n-hexane/isopropanol/diethylamine 75/25/0.1, flow rate = 1.2 mL/min, uv-vis λ =280 nm, t_{R1} = 7.2 min.

Q3: When investigating the reaction order of *Ps*6OMT and CNMT, the authors should identify the compound formed by the CNMT reaction with substrate **3a** and provide the corresponding reference standards. These details should be incorporated into Figure 2a and Supplementary Fig. 3 to make the data more solid.

A3: Thanks for your valuable suggestion. We have identified the compound formed by the CNMT reaction with substrate (*S*)-**3a** by LC-MS, and then updated Figure 2b and Supplementary Fig. 4 as follows:

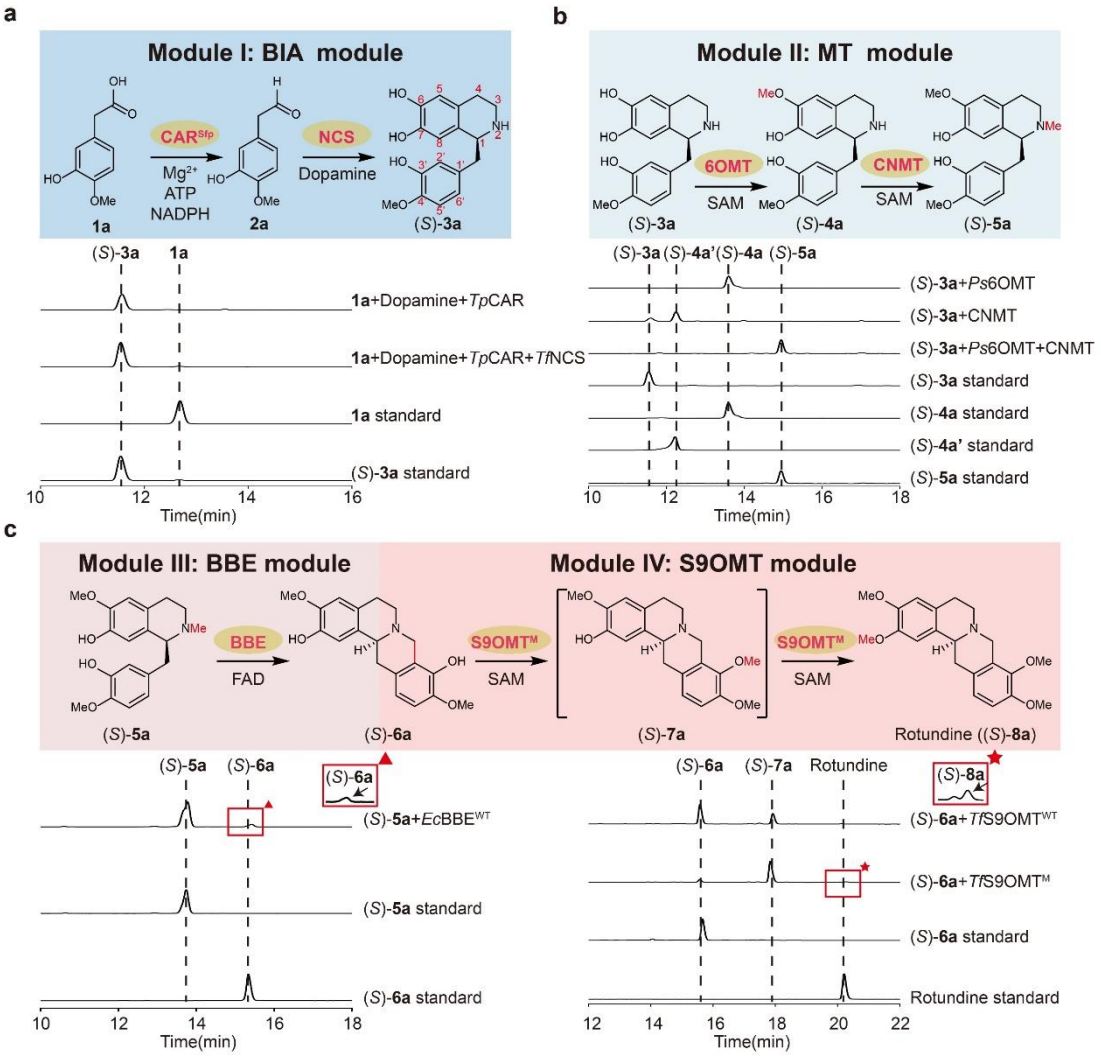

Fig. 2. Establishment of a multi-enzyme cascade reaction to efficiently synthesize Rotundine *in vitro*.

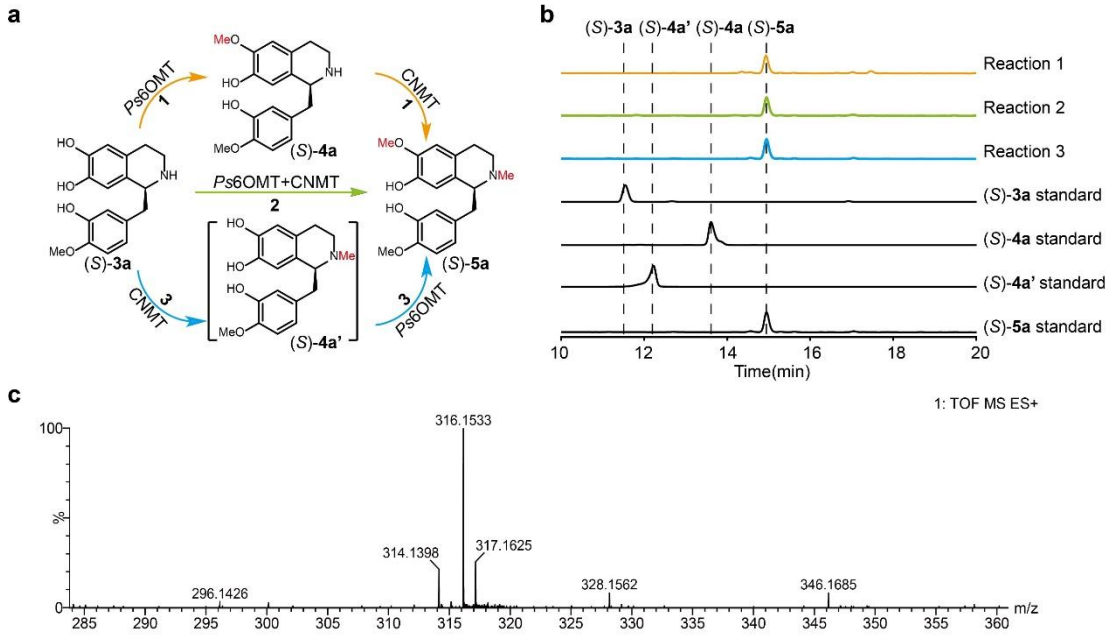

Supplementary Figure 4. Reaction sequence investigation of *Ps*6OMT and CNMT for the substrate (*S*)-3a and HRMS spectrum of (*S*)-4a'.

Q4: A prior study (DOI: 10.1021/acssuschemeng.3c08493) reported that F398W-I431F mutations in *Am*BBE1 significantly improved catalytic activity, achieving nearly 100% conversion rates. The authors are suggested to introduce these mutations into *Ec*BBE and compare the results with the R354W mutant. Will there be synergistic or additive effect among these mutations? Additionally, the method used to identify conserved amino acids (Line 264) should be explicitly detailed.

A4: Thanks for your valuable suggestion. In this study, the EcBBE is from other species. According to the alignment of sequences, the corresponding site of *Am*BBE-F398 is *Ec*BBE-F386 and that of *Am*BBE-I431 is *Ec*BBE-I419. In this work, *Ec*BBE-F386W also showed a 5-fold increase in catalytic activity for converting (*S*)-**5a** to (*S*)-**6a** compared to wild-type *Ec*BBE (*Ec*BBE^{WT}), as well as *Ec*BBE-I419F showed a 125-fold increase. However, in our study, the double mutant *Ec*BBE-R354W/I419F showed no enzymatic activity towards (*S*)-**5a**. Considering the enzymatic activity of *Ec*BBE-I419 is slightly lower than that of *Ec*BBE-R354W, we still chose *Ec*BBE-R354W mutant for subsequent study.

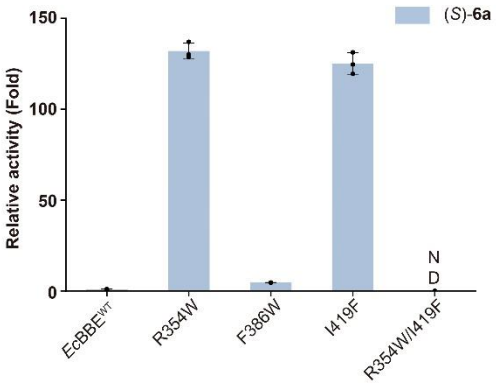

In addition, the method used to identify conserved amino acids was described in figure legend of Supplementary Fig. 19, which has been attached as follows:

"A total of 100 sequences exhibiting at least 50% identity with *Ec*BBE were generated using BLAST tools available through NCBI. Sequence alignment was conducted using BioEdit, and the regions of interest were visualized using WebLogo."

Q5: Minor Points

Line 102: “C3 and C4” should be “C3’ and C4’”.

A5: Thanks for your careful and professional review. We have changed “C3 and C4” to “C3’ and C4’”.

Q6: Line 228: “E. coli” should be italicize

A6: Thanks for your careful and elaborative review. We have corrected the format of “*E. coli*”, and checked throughout the manuscript and Supplementary Information.

Response to reviewers:

To Reviewer #1 (Remarks to the Author):

This revision and additional information provided have addressed my concerns. I believe this work will contribute significantly to the industrial production of protoberberine alkaloid.

A: We greatly appreciate your positive evaluations and valuable suggestions, which help us improve the quality of this manuscript. Here we prepared this point-to-point response to your concerns, which have been completely addressed, and highlighted the changes in red in the revised manuscript.

Minor comment

Q1: Line 109, C3' and C4' should be C3′ and C4′.

A1: Thanks for your careful and professional review to raise this issue. We have changed " C3' and C4' " to "C3′ and C4′", and checked throughout the manuscript and Supplementary Information.

To Reviewer #2 (Remarks to the Author):

The authors have added more data and addresses most of my comments. However, there are still some questions remain unsolved.

A: We greatly appreciate your positive evaluations and valuable suggestions, which help us further improve the quality of this manuscript. Here we prepared this point-to-point response to your concerns, which have been completely addressed, and highlighted the changes in red in the revised manuscript.

Q1: As the authors mentioned, previous study (ACS Catal. 10, 4497-4509 (2020)) clearly demonstrated that leucine at position 111 was more effective than alanine for conversion of (S)-7a. What was the rational for performing the L111A mutation?

A1: Thanks for your constructive advice on the mutation of *Tf*S9OMT. Considering that the catalytic activity of *Tf*S9OMT-L111A mutant was only tested *in vivo* in previous study

(Valentic, T. R. et al. *ACS Catal.* **10**, 4497-4509 (2020)), we further clarified the change of the catalytic activity of this mutant during *in vitro* assays. Meanwhile, in the docking results of (*S*)-**7a** and *Tf*S9OMT^{M}, position 111 was located within 4.0 Å surrounding the D-ring of (*S*)-**7a.** Therefore, for the logic and integrity of the directed evolution strategy, we still tested the activity of the L111A mutant *in vitro*, and the results were consistent with previous studies that the catalytic activity was decreased. To avoid misunderstanding, we amended the corresponding description in the manuscript as follows:

"To reduce the steric hindrance around the D-ring caused by the methoxy group, amino acids within 4.0 Å of *Tf*S9OMT^{M} surrounding the D-ring of (*S*)-**7a** were mutated to small (alanine and glycine) or medium-sized (leucine) residues, including L13, G14, S16, L111, T115, N297, T300, P301 and L304 (Fig. 5c, Supplementary Fig. 28)."

Q2: Moreover, in Fig 5c, most residues were mutated to either A or G, yet some were only mutated to A. What was the reason for this selective mutation approach? A more detailed explanation of the methodology or rationale behind these choices would be valuable for protein engineering efforts.

A2: We apologize for the unclear presentation of Fig. 5c. In fact, we mutated and tested all the amino acids within 4.0 Å of *Tf*S9OMT^{M} surrounding the D-ring of (*S*)-**7a**, including L13, G14, S16, L111, T115, N297, T300, P301 and L304, to alanine, glycine and leucine. Considering the aesthetics of typographic, we only showed alanine mutations of each site and few mutations with increased activity in Fig. 5c, and the rest of the results were shown in Supplementary Fig. 28. To avoid misunderstandings, we supplemented the complete set of results for each site that was mutated to alanine, glycine or leucine in Supplementary Fig. 28 as follows:

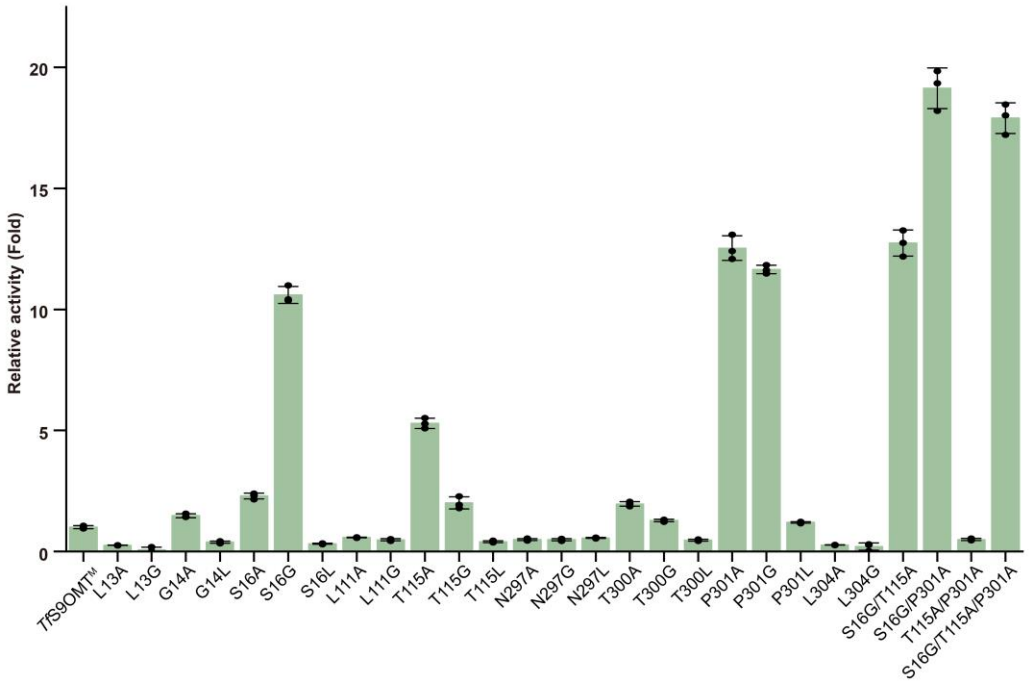

Supplementary Figure 28. Relative activity of all mutants of *Tf*S9OMT^{M} toward (*S*)-6a *in vitro*. The relative activity is defined as the ratio of the Rotundine titer of *Tf*S9OMT^{M} mutants to that of *Tf*S9OMT^{M}.

Q3: The molecular mechanism of the R354W mutation's effect on EcBBE activity was not entirely convincing. The authors mentioned that the distance between the C2' carbon and the carbon atom on the N-methyl group of (S)-5a decreased. Could you provide further clarification, such as showing how this residue interact with these atoms (the C2' carbon and the carbon atom on the N-methyl group of (S)-5a)?

A3: Thanks for your professional comment. We first investigated the residue W354 for its interactions with other residues or the substrate. Based on our analysis of the MD simulation trajectories, residue R354 does not directly interact with the C2' carbon and the carbon atom on the *N*-methyl group of (*S*)-**5a**, but interacts with the substrate indirectly through the residue D352, which is positioned between R354 and the substrate. In the MD simulation of the wild-type (WT) enzyme, R354 and D352 collectively stabilize the substrate in a rigid conformation by forming a hydrogen bond between the hydroxyl group of the substrate and the carbonyl group of D352 (Supplementary Fig. 22c, 24a). However, for the mutant R354W, the hydrogen bonds between the substrate and D352 is significantly reduced, which could be observed in the heat map of hydrogen-bond interactions

(Supplementary Fig. 24b). The change of hydrogen-bond interactions caused by this mutation might thereby enable a more favorable conformation for the carbon atom on the *N*-methyl group of (*S*)-**5a** to approach the C2' carbon of the substrate during the second C-C coupling process (Supplementary Fig. 23c).

Moreover, we have also investigated the mechanism for the improved activity of mutation R354W in the three processes (deprotonation, C-C coupling, and hydride transfer processes), showing that the mutation of R354W improved not only the second C-C coupling process, but also the first deprotonation process. While the third hydride transfer process might not be affected significantly. The corresponding results are also detailly listed in **Answer to Q4**.

We have added the corresponding description and results in the revised manuscript and Supporting Information, which are listed as follows.

"Based on the results of molecular dynamics (MD) simulations, it suggests that this mutation enhances the protein stability, strengthens the substrate-binding by changing hydrogen bond network, and improvesthe activity of deprotonation and C-C coupling processes, in which both the distance between the carboxyl group of E417 and C3′ OH group of (S)-**5a** (from 2.41 Å to 1.84 Å) and the distance between the C2′ carbon and the carbon atom on the N-methyl group of (S)-**5a** (from 4.19 Å to 3.64 Å) are shortened to favor the berberine bridge formation (Supplementary Fig. 22, 23, 24)."

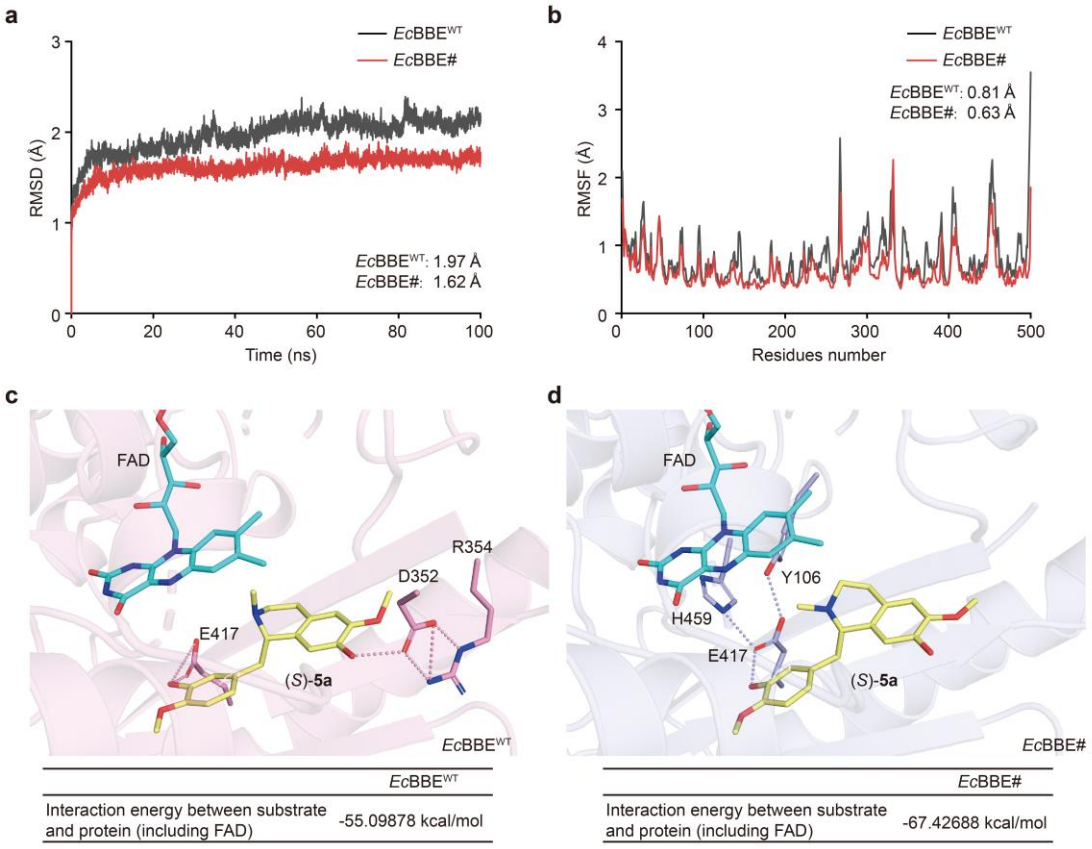

	*Ec*BBE^{WT}
Interaction energy between substrate and protein (including FAD)	-55.09878 kcal/mol

	*Ec*BBE#
Interaction energy between substrate and protein (including FAD)	-67.42688 kcal/mol

Supplementary Figure 22. Molecular dynamics simulation analysis and representative snapshot for wild type *Ec*BBE and mutant *Ec*BBE#. a Root mean square deviation (RMSD). **b** Root mean square fluctuation (RMSF). **c** The representative snapshot of *Ec*BBE^{WT}. **d** The representative snapshot of *Ec*BBE#. Light pink or light blue dotted lines: hydrogen-bonds.

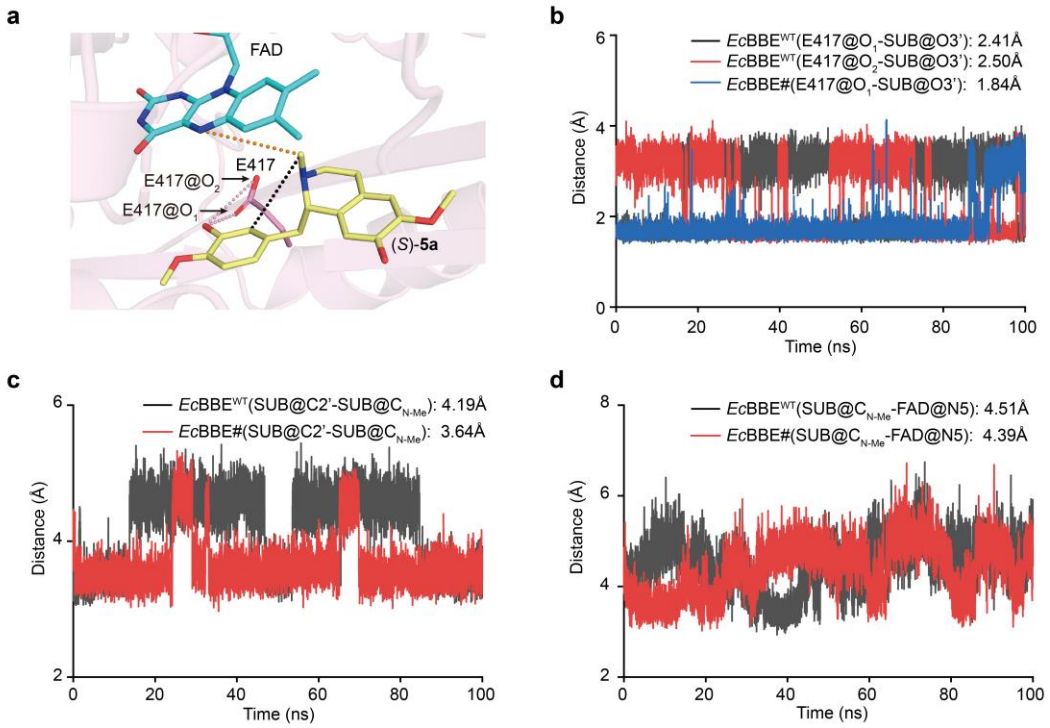

Supplementary Figure 23. Important distance investigations of *Ec*BBE^{WT} or *Ec*BBE# in MD simulations. a Schematic representation of the three interatomic distances. Light pink dotted lines: the distance between the C3′ OH group of (*S*)-**5a** and two oxygen atoms in the carboxyl group of E417 in *Ec*BBE; Black dotted lines: the distance between the C2′ carbon and the carbon atom on the *N*-methyl group of (*S*)-**5a**; Orange dotted lines: the distance between the carbon atom on the *N*-methyl group of (*S*)-**5a** and N5 atom of FAD. **b** The distance between the C3′ OH group of (*S*)-**5a** and two oxygen atoms in the carboxyl group of E417 in *Ec*BBE. **c** The distance between the C2′ carbon and the carbon atom on the *N*-methyl group of (*S*)-**5a**. **d** The distance between the carbon atom on the *N*-methyl group of (*S*)-**5a** and N5 atom of FAD.

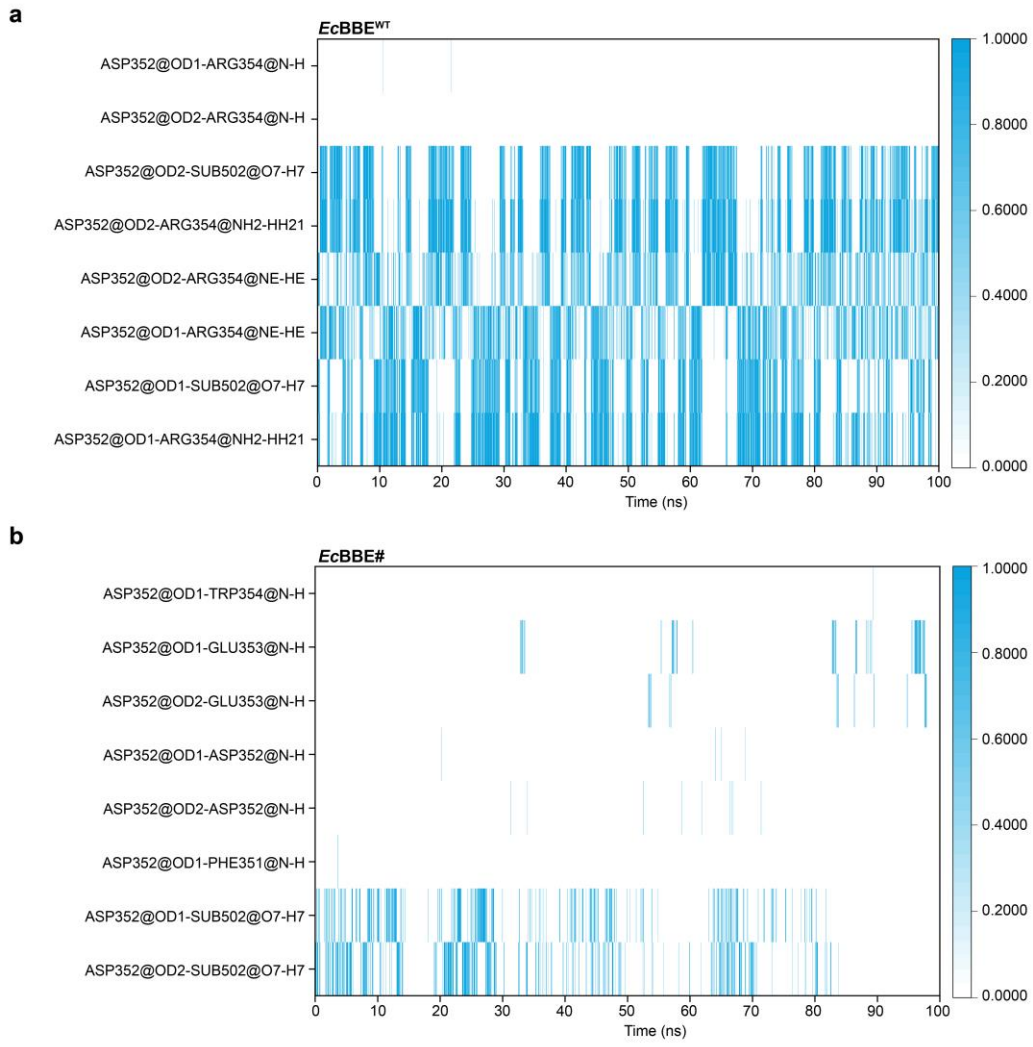

Supplementary Figure 24. Heat map of hydrogen-bond interactions between (*S*)-5a and *Ec*BBE^{WT} (a) or *Ec*BBE# (b) in MD simulations.

Q4: Additionaly, it was shown that the reaction initated by deprotonation of the C3' OH by E417 (Nat Chem Biol, 2008). How does the R354W mutation influence this deprotonation process?

A4: Thanks for your valuable question. According to previous study (Winkler, A. *et al. Nat. Chem. Biol.* **4**, 739-741 (2008)), the berberine bridge formation could be divided into three processes: 1) deprotonation of the C3' OH group by the carboxyl group of E417 which initiated the reaction; 2) C-C coupling through S_N2-type attack onto the *N*-methyl group resulting in the formation of the berberine bridge; 3) hydride transfer from the methyl group to the flavin N5 position leading to a two-electron reduction of the cofactor.

To further explore the effect of the mutation on these reaction process, we examined the MD simulations of both WT and R354W variants, extracted representative snapshots, and observed significant changes in the polar interactions surrounding (*S*)-**5a** (Supplementary Fig. 22, 23). Firstly, in the representative snapshot of the R354W simulation, residues Y106 and H459 collectively stabilize the substrate by forming new hydrogen bonds with the carbonyl group of E417 for better substrate binding (-67.43 kcal/mol) than *Ec*BBE^{WT} (-55.10 kcal/mol) (Supplementary Fig. 22c, 22d). Meanwhile, the altered hydrogen bond network shortened the distance between the C3′ OH group of (*S*)-**5a** and the carboxyl group of E417 (from 2.41 or 2.50 Å to 1.84 Å), which could facilitate the E417-driven deprotonation and thus improve the catalytic efficiency of *Ec*BBE-R354W mutant (Supplementary Fig. 23b).

Moreover, we also studied the following C-C coupling and hydride transfer processes. Secondly in the C-C coupling process, the *Ec*BBE-R354W mutant alleviated the rigid conformation of the substrate caused by the disappeared hydrogen bond network between D352, R354 and the (*S*)-**5a** in *Ec*BBE^{WT} (Supplementary Fig. 22c, 22d, 24), shortening the distance between the C2' carbon and the carbon atom on the *N*-methyl group of (*S*)-**5a** (Supplementary Fig. 23c) to favor the formation of the berberine bridge. In the third hydride transfer process, the distance between the carbon atom on the *N*-methyl group of (*S*)-**5a** and N5 atom of FAD were almost the same in *Ec*BBE^{WT} and *Ec*BBE-R354W (Supplementary Fig. 23d), indicating that the hydride transfer process might not be affected significantly.

Overall, the *Ec*BBE-R354W mutant enhanced the catalytic activity mainly due to the decreased substrate-binding energy, the improved deprotonation and C-C coupling process, according to the shorter distance between the C3′ OH group of (*S*)-**5a** and two

oxygen atoms in the carboxyl group of E417, and the shorter distance between the C2′ carbon and the carbon atom on the *N*-methyl group of (*S*)-**5a**.

We have added the corresponding description and results in the revised manuscript and Supporting Information, which are listed as follows.

"Based on the results of molecular dynamics (MD) simulations, it suggests that this mutation enhances the protein stability, strengthens the substrate-binding by changing hydrogen bond network, and improvesthe activity of deprotonation and C-C coupling processes, in which both the distance between the carboxyl group of E417 and C3′ OH group of (S)-**5a** (from 2.41 Å to 1.84 Å) and the distance between the C2′ carbon and the carbon atom on the N-methyl group of (S)-**5a** (from 4.19 Å to 3.64 Å) are shortened to favor the berberine bridge formation (Supplementary Fig. 22, 23, 24)."

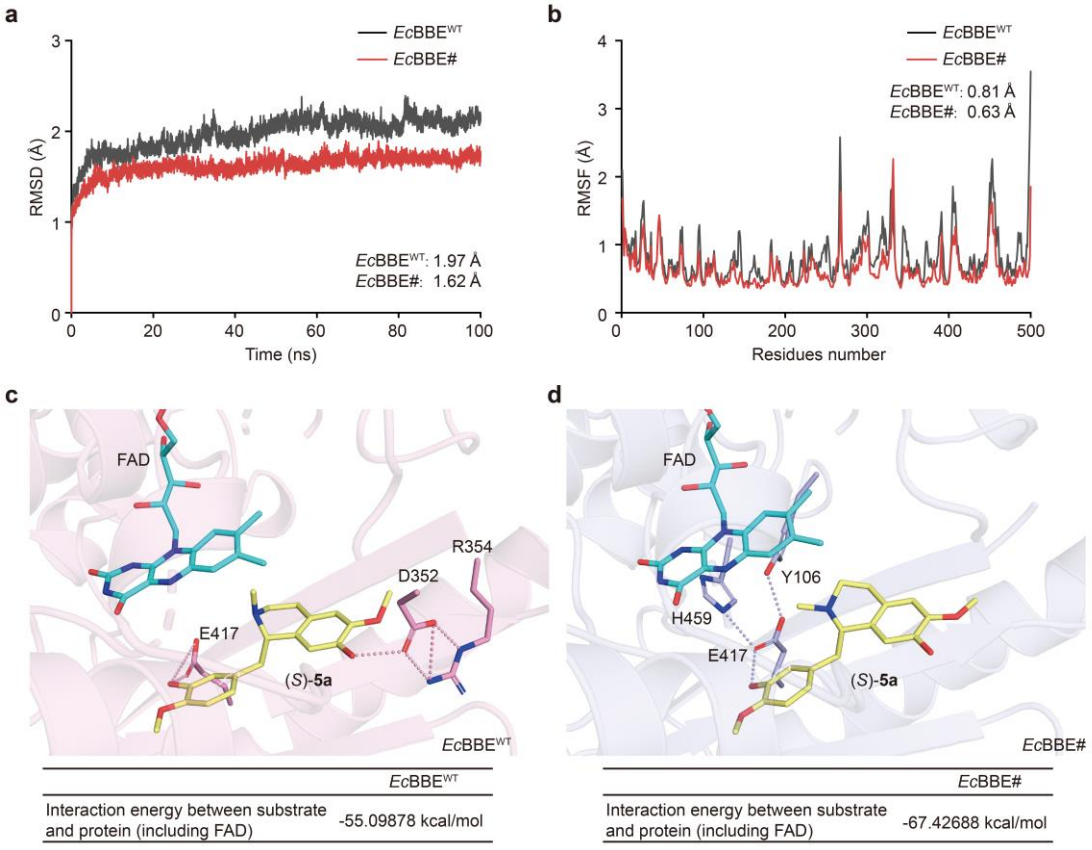

	*Ec*BBE^{WT}
Interaction energy between substrate and protein (including FAD)	-55.09878 kcal/mol

	*Ec*BBE#
Interaction energy between substrate and protein (including FAD)	-67.42688 kcal/mol

Supplementary Figure 22. Molecular dynamics simulation analysis and representative snapshot for wild type *Ec*BBE and mutant *Ec*BBE#. a Root mean square deviation (RMSD). **b** Root mean square fluctuation (RMSF). **c** The representative snapshot of *Ec*BBE^{WT}. **d** The representative snapshot of *Ec*BBE#. Light pink or light blue

dotted lines: hydrogen-bonds.

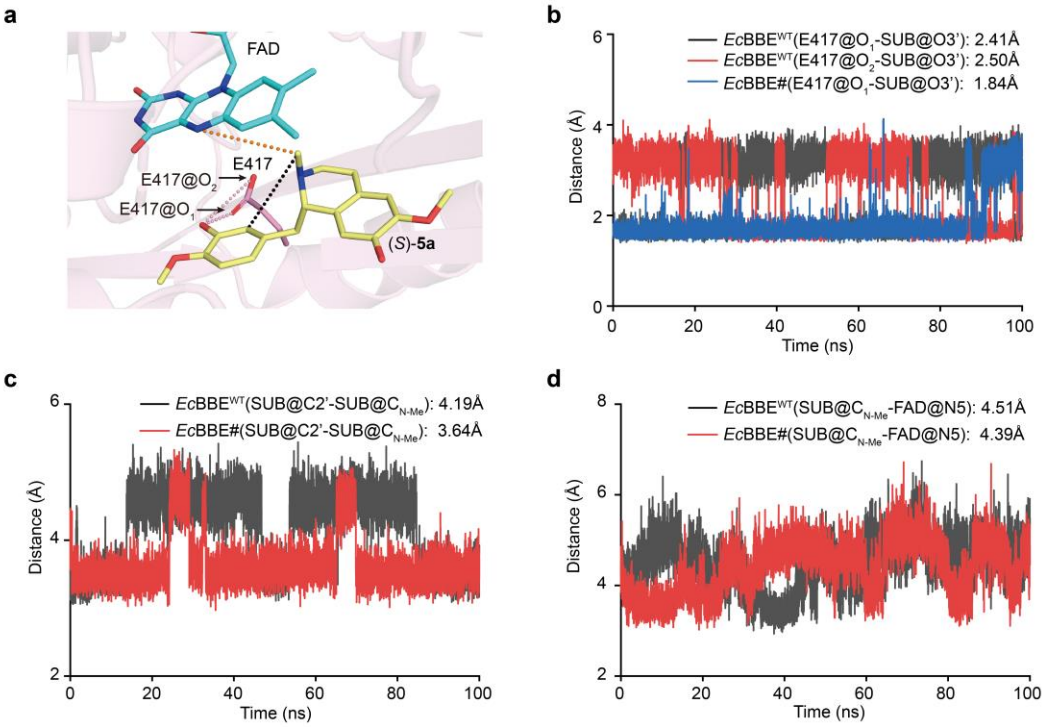

Supplementary Figure 23. Important distance investigations of *Ec*BBE^{WT} or *Ec*BBE# in MD simulations. a Schematic representation of the three interatomic distances. Light pink dotted lines: the distance between the C3′ OH group of (*S*)-**5a** and two oxygen atoms in the carboxyl group of E417 in *Ec*BBE; Black dotted lines: the distance between the C2′ carbon and the carbon atom on the *N*-methyl group of (*S*)-**5a**; Orange dotted lines: the distance between the carbon atom on the *N*-methyl group of (*S*)-**5a** and N5 atom of FAD. **b** The distance between the C3′ OH group of (*S*)-**5a** and two oxygen atoms in the carboxyl group of E417 in *Ec*BBE. **c** The distance between the C2′ carbon and the carbon atom on the *N*-methyl group of (*S*)-**5a**. **d** The distance between the carbon atom on the *N*-methyl group of (*S*)-**5a** and N5 atom of FAD.

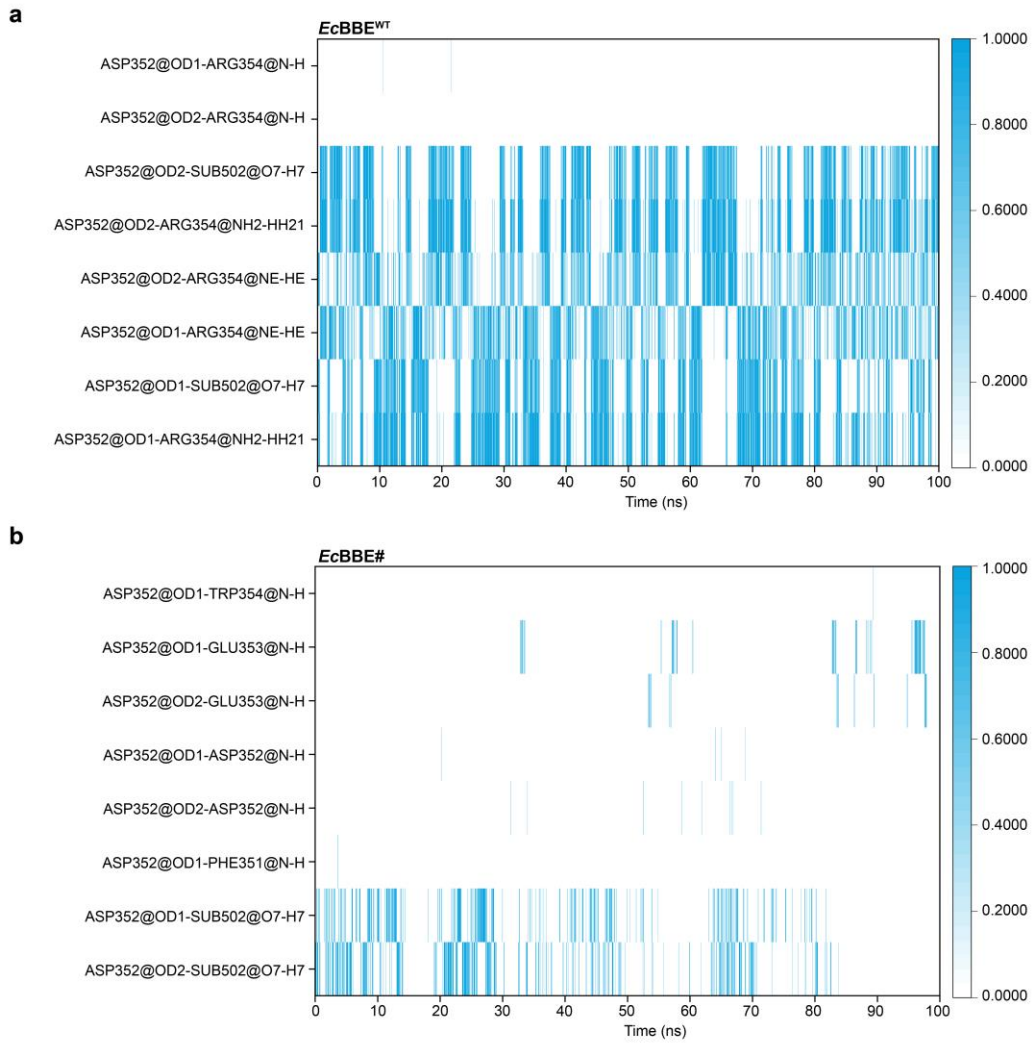

Supplementary Figure 24. Heat map of hydrogen-bond interactions between (*S*)-5a and *Ec*BBE^{WT} (a) or *Ec*BBE# (b) in MD simulations.

To Reviewer #3 (Remarks to the Author):

The authors have done a nice job in addressing all the reviewers' concerns.

A: We would like to thank again the reviewer for the thoughtful comments and constructive suggestions, which help us improve the quality of this manuscript.

Response to reviewers:

To Reviewer #1 (Remarks to the Author):

This revision and additional information provided have addressed my concerns. I believe this work will contribute significantly to the industrial production of protoberberine alkaloid.

A: We greatly appreciate your positive evaluations and valuable suggestions, which help us improve the quality of this manuscript. Here we prepared this point-to-point response to your concerns, which have been completely addressed, and highlighted the changes in red in the revised manuscript.

Minor comment

Q1: Line 109, C3' and C4' should be C3′ and C4′.

A1: Thanks for your careful and professional review to raise this issue. We have changed " C3' and C4' " to "C3′ and C4′", and checked throughout the manuscript and Supplementary Information.

To Reviewer #2 (Remarks to the Author):

The authors have added more data and addresses most of my comments. However, there are still some questions remain unsolved.

A: We greatly appreciate your positive evaluations and valuable suggestions, which help us further improve the quality of this manuscript. Here we prepared this point-to-point response to your concerns, which have been completely addressed, and highlighted the changes in red in the revised manuscript.

Q1: As the authors mentioned, previous study (ACS Catal. 10, 4497-4509 (2020)) clearly demonstrated that leucine at position 111 was more effective than alanine for conversion of (S)-7a. What was the rational for performing the L111A mutation?

A1: Thanks for your constructive advice on the mutation of *Tf*S9OMT. Considering that the catalytic activity of *Tf*S9OMT-L111A mutant was only tested *in vivo* in previous study

(Valentic, T. R. et al. *ACS Catal.* **10**, 4497-4509 (2020)), we further clarified the change of the catalytic activity of this mutant during *in vitro* assays. Meanwhile, in the docking results of (*S*)-**7a** and *Tf*S9OMT^{M}, position 111 was located within 4.0 Å surrounding the D-ring of (*S*)-**7a.** Therefore, for the logic and integrity of the directed evolution strategy, we still tested the activity of the L111A mutant *in vitro*, and the results were consistent with previous studies that the catalytic activity was decreased. To avoid misunderstanding, we amended the corresponding description in the manuscript as follows:

"To reduce the steric hindrance around the D-ring caused by the methoxy group, amino acids within 4.0 Å of *Tf*S9OMT^{M} surrounding the D-ring of (*S*)-**7a** were mutated to small (alanine and glycine) or medium-sized (leucine) residues, including L13, G14, S16, L111, T115, N297, T300, P301 and L304 (Fig. 5c, Supplementary Fig. 28)."

Q2: Moreover, in Fig 5c, most residues were mutated to either A or G, yet some were only mutated to A. What was the reason for this selective mutation approach? A more detailed explanation of the methodology or rationale behind these choices would be valuable for protein engineering efforts.

A2: We apologize for the unclear presentation of Fig. 5c. In fact, we mutated and tested all the amino acids within 4.0 Å of *Tf*S9OMT^{M} surrounding the D-ring of (*S*)-**7a**, including L13, G14, S16, L111, T115, N297, T300, P301 and L304, to alanine, glycine and leucine. Considering the aesthetics of typographic, we only showed alanine mutations of each site and few mutations with increased activity in Fig. 5c, and the rest of the results were shown in Supplementary Fig. 28. To avoid misunderstandings, we supplemented the complete set of results for each site that was mutated to alanine, glycine or leucine in Supplementary Fig. 28 as follows:

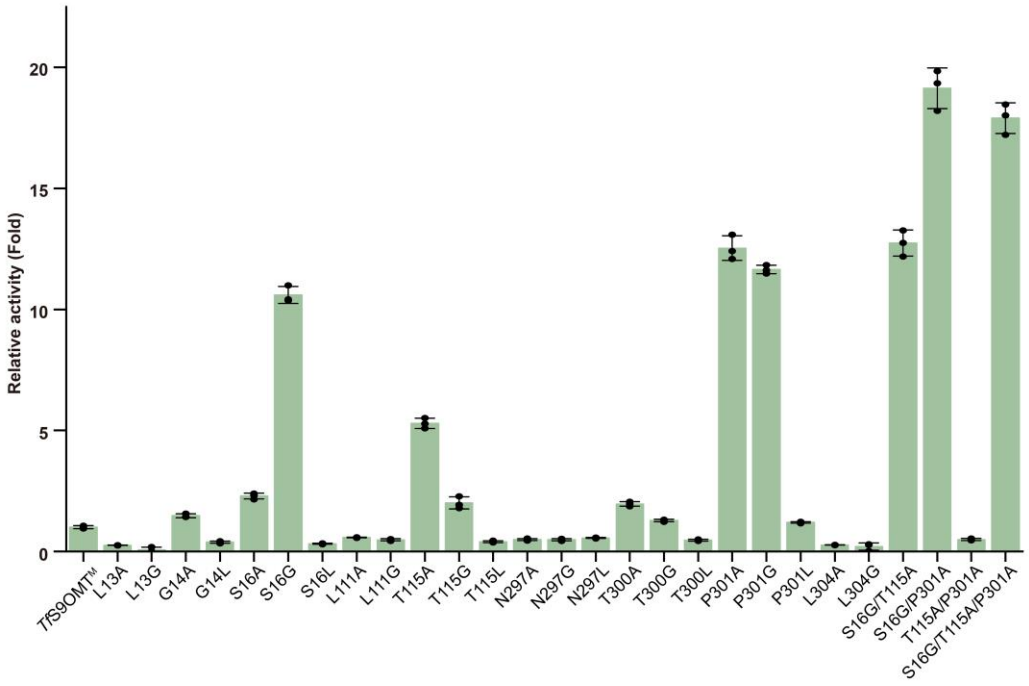

Supplementary Figure 28. Relative activity of all mutants of *Tf*S9OMT^{M} toward (*S*)-6a *in vitro*. The relative activity is defined as the ratio of the Rotundine titer of *Tf*S9OMT^{M} mutants to that of *Tf*S9OMT^{M}.

Q3: The molecular mechanism of the R354W mutation's effect on EcBBE activity was not entirely convincing. The authors mentioned that the distance between the C2' carbon and the carbon atom on the N-methyl group of (S)-5a decreased. Could you provide further clarification, such as showing how this residue interact with these atoms (the C2' carbon and the carbon atom on the N-methyl group of (S)-5a)?

A3: Thanks for your professional comment. We first investigated the residue W354 for its interactions with other residues or the substrate. Based on our analysis of the MD simulation trajectories, residue R354 does not directly interact with the C2' carbon and the carbon atom on the *N*-methyl group of (*S*)-**5a**, but interacts with the substrate indirectly through the residue D352, which is positioned between R354 and the substrate. In the MD simulation of the wild-type (WT) enzyme, R354 and D352 collectively stabilize the substrate in a rigid conformation by forming a hydrogen bond between the hydroxyl group of the substrate and the carbonyl group of D352 (Supplementary Fig. 22c, 24a). However, for the mutant R354W, the hydrogen bonds between the substrate and D352 is significantly reduced, which could be observed in the heat map of hydrogen-bond interactions

(Supplementary Fig. 24b). The change of hydrogen-bond interactions caused by this mutation might thereby enable a more favorable conformation for the carbon atom on the *N*-methyl group of (*S*)-**5a** to approach the C2' carbon of the substrate during the second C-C coupling process (Supplementary Fig. 23c).

Moreover, we have also investigated the mechanism for the improved activity of mutation R354W in the three processes (deprotonation, C-C coupling, and hydride transfer processes), showing that the mutation of R354W improved not only the second C-C coupling process, but also the first deprotonation process. While the third hydride transfer process might not be affected significantly. The corresponding results are also detailly listed in **Answer to Q4**.

We have added the corresponding description and results in the revised manuscript and Supporting Information, which are listed as follows.

"Based on the results of molecular dynamics (MD) simulations, it suggests that this mutation enhances the protein stability, strengthens the substrate-binding by changing hydrogen bond network, and improvesthe activity of deprotonation and C-C coupling processes, in which both the distance between the carboxyl group of E417 and C3′ OH group of (S)-**5a** (from 2.41 Å to 1.84 Å) and the distance between the C2′ carbon and the carbon atom on the N-methyl group of (S)-**5a** (from 4.19 Å to 3.64 Å) are shortened to favor the berberine bridge formation (Supplementary Fig. 22, 23, 24)."

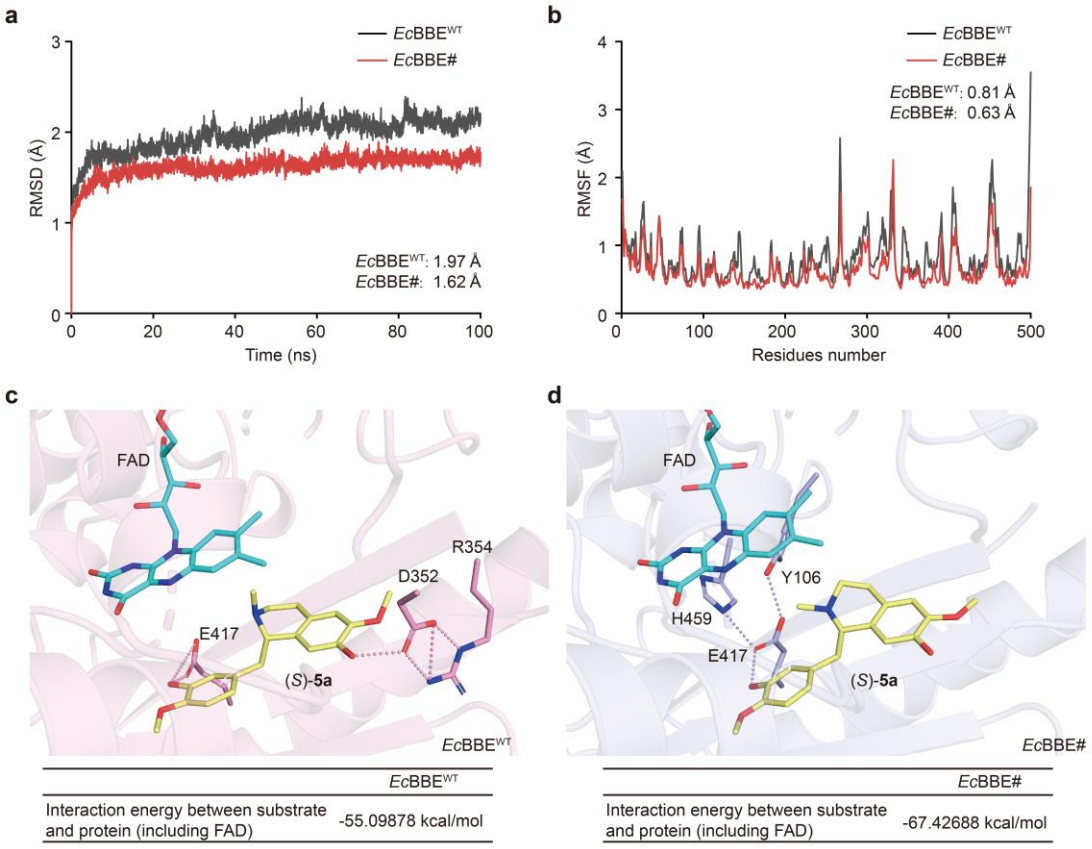

	*Ec*BBE^{WT}
Interaction energy between substrate and protein (including FAD)	-55.09878 kcal/mol

	*Ec*BBE#
Interaction energy between substrate and protein (including FAD)	-67.42688 kcal/mol

Supplementary Figure 22. Molecular dynamics simulation analysis and representative snapshot for wild type *Ec*BBE and mutant *Ec*BBE#. a Root mean square deviation (RMSD). **b** Root mean square fluctuation (RMSF). **c** The representative snapshot of *Ec*BBE^{WT}. **d** The representative snapshot of *Ec*BBE#. Light pink or light blue dotted lines: hydrogen-bonds.

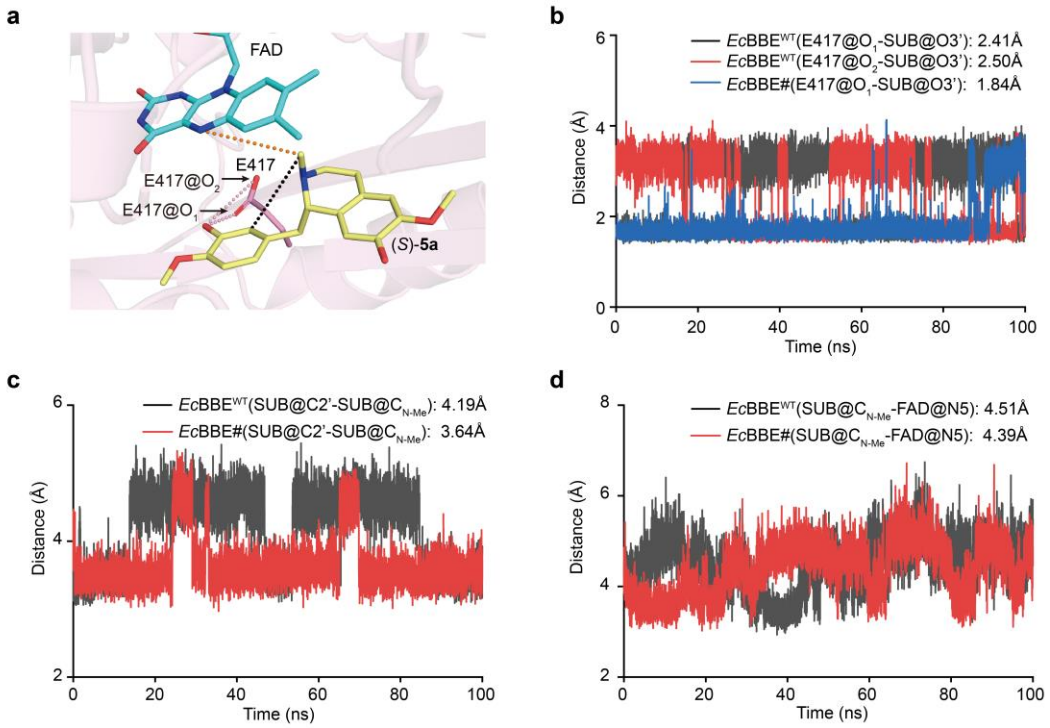

Supplementary Figure 23. Important distance investigations of *Ec*BBE^{WT} or *Ec*BBE# in MD simulations. a Schematic representation of the three interatomic distances. Light pink dotted lines: the distance between the C3′ OH group of (*S*)-**5a** and two oxygen atoms in the carboxyl group of E417 in *Ec*BBE; Black dotted lines: the distance between the C2′ carbon and the carbon atom on the *N*-methyl group of (*S*)-**5a**; Orange dotted lines: the distance between the carbon atom on the *N*-methyl group of (*S*)-**5a** and N5 atom of FAD. **b** The distance between the C3′ OH group of (*S*)-**5a** and two oxygen atoms in the carboxyl group of E417 in *Ec*BBE. **c** The distance between the C2′ carbon and the carbon atom on the *N*-methyl group of (*S*)-**5a**. **d** The distance between the carbon atom on the *N*-methyl group of (*S*)-**5a** and N5 atom of FAD.

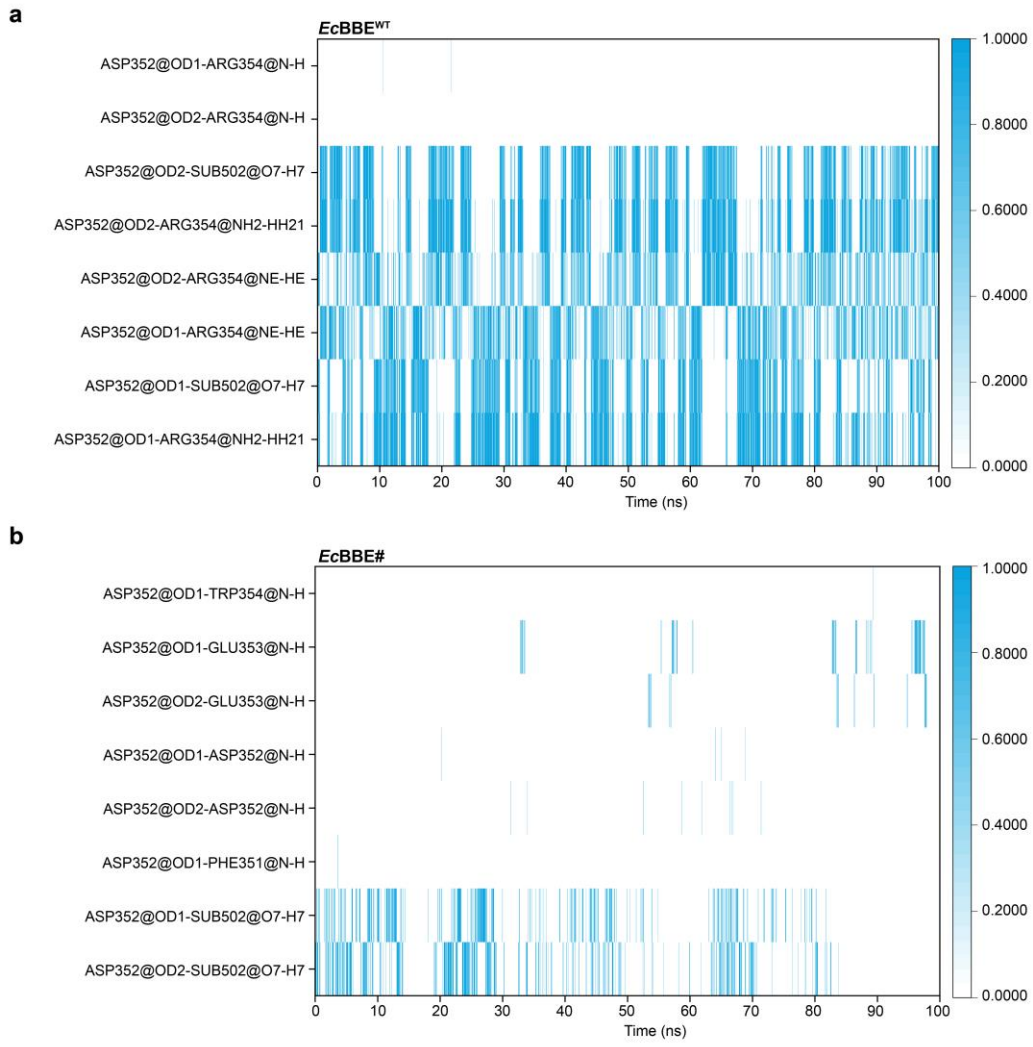

Supplementary Figure 24. Heat map of hydrogen-bond interactions between (*S*)-5a and *Ec*BBE^{WT} (a) or *Ec*BBE# (b) in MD simulations.

Q4: Additionaly, it was shown that the reaction initated by deprotonation of the C3' OH by E417 (Nat Chem Biol, 2008). How does the R354W mutation influence this deprotonation process?

A4: Thanks for your valuable question. According to previous study (Winkler, A. *et al. Nat. Chem. Biol.* **4**, 739-741 (2008)), the berberine bridge formation could be divided into three processes: 1) deprotonation of the C3' OH group by the carboxyl group of E417 which initiated the reaction; 2) C-C coupling through S_N2-type attack onto the *N*-methyl group resulting in the formation of the berberine bridge; 3) hydride transfer from the methyl group to the flavin N5 position leading to a two-electron reduction of the cofactor.

To further explore the effect of the mutation on these reaction process, we examined the MD simulations of both WT and R354W variants, extracted representative snapshots, and observed significant changes in the polar interactions surrounding (*S*)-**5a** (Supplementary Fig. 22, 23). Firstly, in the representative snapshot of the R354W simulation, residues Y106 and H459 collectively stabilize the substrate by forming new hydrogen bonds with the carbonyl group of E417 for better substrate binding (-67.43 kcal/mol) than *Ec*BBE^{WT} (-55.10 kcal/mol) (Supplementary Fig. 22c, 22d). Meanwhile, the altered hydrogen bond network shortened the distance between the C3′ OH group of (*S*)-**5a** and the carboxyl group of E417 (from 2.41 or 2.50 Å to 1.84 Å), which could facilitate the E417-driven deprotonation and thus improve the catalytic efficiency of *Ec*BBE-R354W mutant (Supplementary Fig. 23b).

Moreover, we also studied the following C-C coupling and hydride transfer processes. Secondly in the C-C coupling process, the *Ec*BBE-R354W mutant alleviated the rigid conformation of the substrate caused by the disappeared hydrogen bond network between D352, R354 and the (*S*)-**5a** in *Ec*BBE^{WT} (Supplementary Fig. 22c, 22d, 24), shortening the distance between the C2' carbon and the carbon atom on the *N*-methyl group of (*S*)-**5a** (Supplementary Fig. 23c) to favor the formation of the berberine bridge. In the third hydride transfer process, the distance between the carbon atom on the *N*-methyl group of (*S*)-**5a** and N5 atom of FAD were almost the same in *Ec*BBE^{WT} and *Ec*BBE-R354W (Supplementary Fig. 23d), indicating that the hydride transfer process might not be affected significantly.

Overall, the *Ec*BBE-R354W mutant enhanced the catalytic activity mainly due to the decreased substrate-binding energy, the improved deprotonation and C-C coupling process, according to the shorter distance between the C3′ OH group of (*S*)-**5a** and two

oxygen atoms in the carboxyl group of E417, and the shorter distance between the C2′ carbon and the carbon atom on the *N*-methyl group of (*S*)-**5a**.

We have added the corresponding description and results in the revised manuscript and Supporting Information, which are listed as follows.

"Based on the results of molecular dynamics (MD) simulations, it suggests that this mutation enhances the protein stability, strengthens the substrate-binding by changing hydrogen bond network, and improvesthe activity of deprotonation and C-C coupling processes, in which both the distance between the carboxyl group of E417 and C3′ OH group of (S)-**5a** (from 2.41 Å to 1.84 Å) and the distance between the C2′ carbon and the carbon atom on the N-methyl group of (S)-**5a** (from 4.19 Å to 3.64 Å) are shortened to favor the berberine bridge formation (Supplementary Fig. 22, 23, 24)."

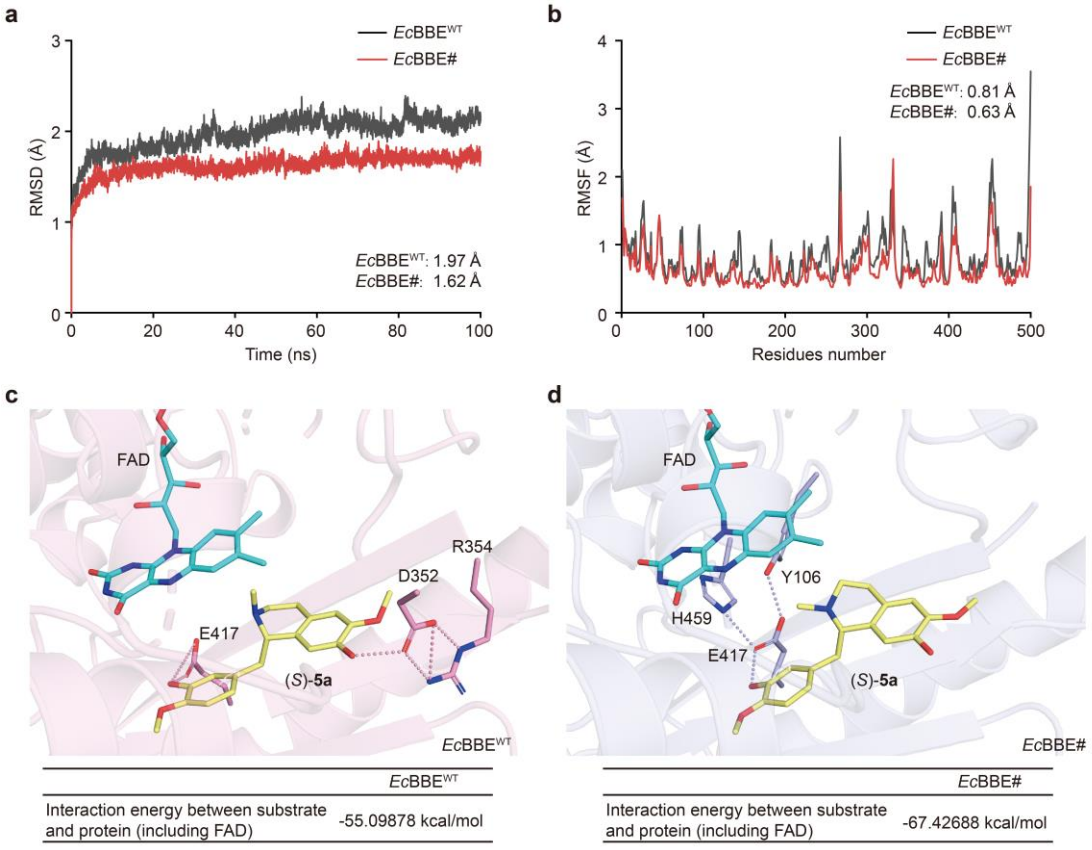

	*Ec*BBE^{WT}
Interaction energy between substrate and protein (including FAD)	-55.09878 kcal/mol

	*Ec*BBE#
Interaction energy between substrate and protein (including FAD)	-67.42688 kcal/mol

Supplementary Figure 22. Molecular dynamics simulation analysis and representative snapshot for wild type *Ec*BBE and mutant *Ec*BBE#. a Root mean square deviation (RMSD). **b** Root mean square fluctuation (RMSF). **c** The representative snapshot of *Ec*BBE^{WT}. **d** The representative snapshot of *Ec*BBE#. Light pink or light blue

dotted lines: hydrogen-bonds.

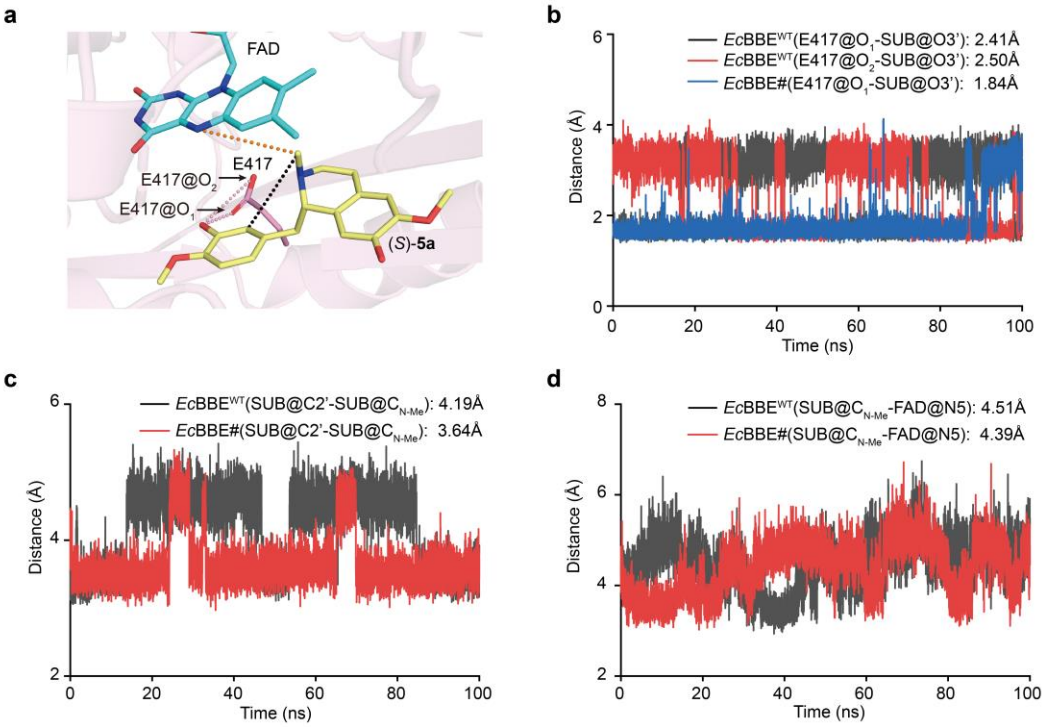

Supplementary Figure 23. Important distance investigations of *Ec*BBE^{WT} or *Ec*BBE# in MD simulations. a Schematic representation of the three interatomic distances. Light pink dotted lines: the distance between the C3′ OH group of (*S*)-**5a** and two oxygen atoms in the carboxyl group of E417 in *Ec*BBE; Black dotted lines: the distance between the C2′ carbon and the carbon atom on the *N*-methyl group of (*S*)-**5a**; Orange dotted lines: the distance between the carbon atom on the *N*-methyl group of (*S*)-**5a** and N5 atom of FAD. **b** The distance between the C3′ OH group of (*S*)-**5a** and two oxygen atoms in the carboxyl group of E417 in *Ec*BBE. **c** The distance between the C2′ carbon and the carbon atom on the *N*-methyl group of (*S*)-**5a**. **d** The distance between the carbon atom on the *N*-methyl group of (*S*)-**5a** and N5 atom of FAD.

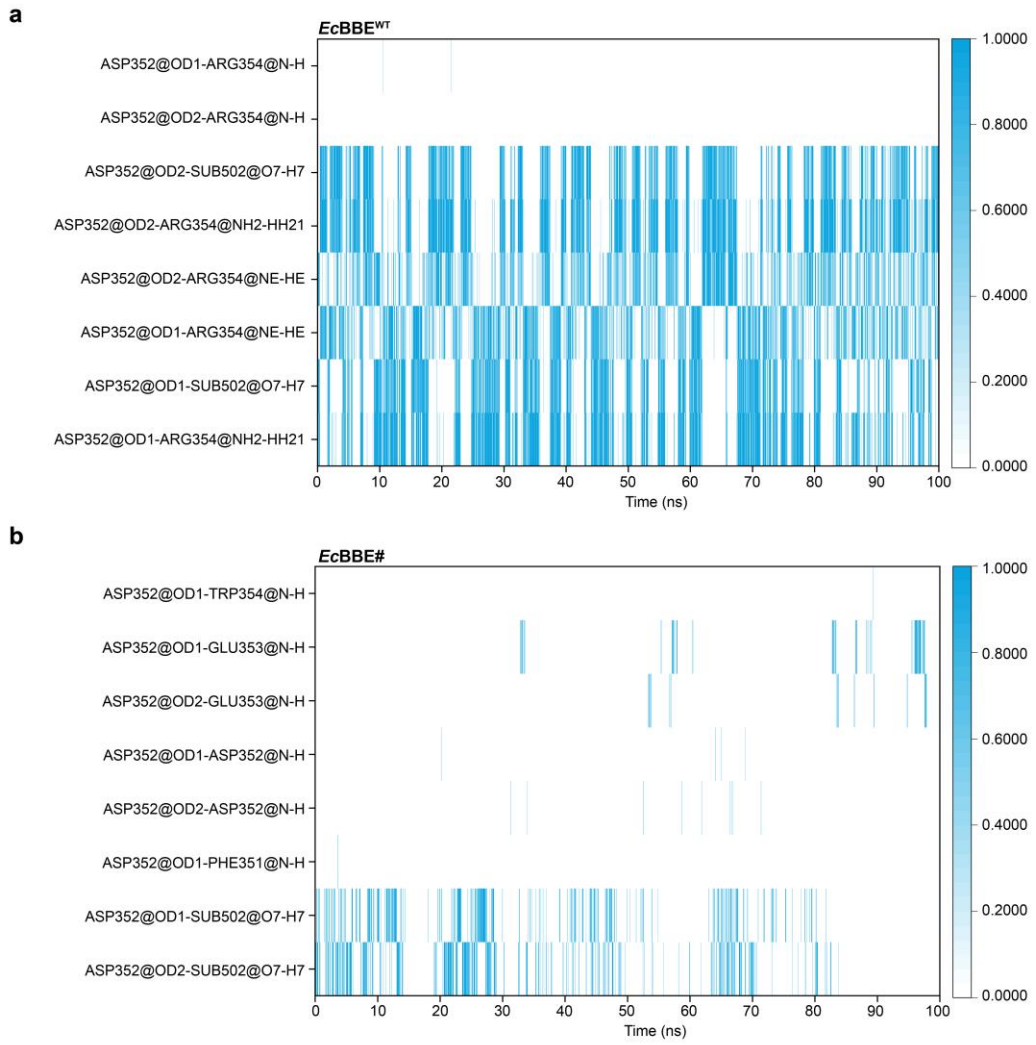

Supplementary Figure 24. Heat map of hydrogen-bond interactions between (*S*)-5a and *Ec*BBE^{WT} (a) or *Ec*BBE# (b) in MD simulations.

To Reviewer #3 (Remarks to the Author):

The authors have done a nice job in addressing all the reviewers' concerns.

A: We would like to thank again the reviewer for the thoughtful comments and constructive suggestions, which help us improve the quality of this manuscript.